HOMOCLINIC BOUNDARY-SADDLE BIFURCATIONS IN NONSMOOTH VECTOR FIELDS

KAMILA DA S. ANDRADE, MIKE R. JEFFREY, RICARDO M. MARTINS,
AND MARCO A. TEIXEIRA

ABSTRACT. In a smooth dynamical system, a homoclinic connection is a closed orbit returning to a saddle equilibrium. Under perturbation, homoclinics are associated with bifurcations of periodic orbits, and with chaos in higher dimensions. Homoclinic connections in nonsmooth systems are complicated by their interaction with discontinuities in their vector fields. A connection may involve a regular saddle outside a discontinuity set, or a pseudo-saddle on a discontinuity set, with segments of the connection allowed to cross or slide along the discontinuity. Even the simplest case, that of connection to a regular saddle that hits a discontinuity as a parameter is varied, is surprisingly complex. Bifurcation diagrams are presented here for non-resonant saddles in the plane, including an example in a forced pendulum.

1. INTRODUCTION

In smooth dynamical systems, a homoclinic orbit is a closed trajectory connecting a saddle equilibrium to itself. Under perturbation the homoclinic orbit can create a limit cycle or, in more than two dimensions, chaos. Homoclinic orbits in nonsmooth systems come in multiple different forms, only the simplest of which have so far been studied. For example, regular saddles with homoclinic orbits that involve segments of sliding along a line of discontinuity, or homoclinics to so-called pseudo-saddles in the sliding dynamics itself, are studied as one parameter bifurcations in [1].

A boundary homoclinic orbit, which involves a regular saddle lying on the discontinuity set of a nonsmooth system, is novel so far as classification, because it involves both a local bifurcation (a saddle lying on the discontinuity set, or a so-called *boundary equilibrium* bifurcation [2]), and a global bifurcation in the form of the homoclinic connection. Its unfolding then involves the transition of the saddle into a pseudo-saddle, and the appearance of not one limit cycle, but multiple. The precise unfolding is surprisingly complex even in two dimensions. The bifurcation diagrams for non-resonant saddles in the plane are derived here, including an example in a pendulum with a discontinuous forcing.

Our interest is in systems of the form

$$(1) \qquad \dot{x} = Z(x) = \begin{cases} X(x) & h(x) \geq 0, \\ Y(x) & h(x) \leq 0, \end{cases}$$

where $h : \mathbb{R}^2 \to \mathbb{R}$ is a smooth function having 0 as a regular value, and $X, Y \in \chi^r$, where χ^r is the set of all C^r vector fields defined in $\mathbb{R}^2$, and χ^r is endowed with the C^r topology.

The righthand side Z is a nonsmooth vector field, which for brevity we may write as $Z = (X, Y)$. Denote by $\Omega^r = \chi^r \times \chi^r$ the set of all nonsmooth vector fields Z endowed with the product topology. The set $\Sigma = \{p \in \mathbb{R}^2;\ h(p) = 0\}$ is called the switching surface and the definition of trajectories follows Filippov's convention, see [3].

Our objective is to study bifurcations of a degenerate cycle passing through a saddle point of X lying on Σ, called a hyperbolic saddle-regular point of Z. We are thus concerned with vector fields $Z = (X, Y) \in \Omega^r$ where X has a hyperbolic saddle point $S_X \in \Sigma$ which is a regular point for Y (meaning Y is non-zero and transverse to Σ at S_X). The stable and unstable manifolds of S_X are transverse to Σ in S_X and the unstable manifold intersects Σ transversely at a point $P_X \in \Sigma \setminus \{S_X\}$. The trajectory of Y passing through P_X intersects Σ transversely at S_X and P_X. An example of this kind of cycle is illustrated in figure 1.
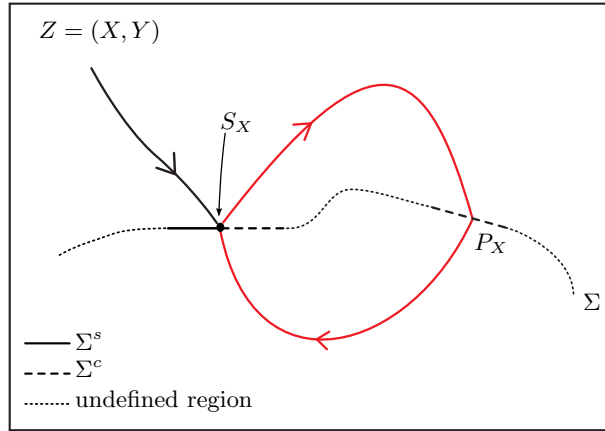

FIGURE 1. A degenerate cycle passing through a saddle-regular point. Σ^s, Σ^c are, respectively, the sliding and crossing regions.

An overview of concepts and definitions are given in Section 2. The setting of the problem and the study of the first return map for the degenerate cycle are given in Section 3. In Section 4 the main results and the corresponding bifurcation diagrams are presented. Section 5 presents models having a degenerate cycle through resonant saddle-regular point. In Section 6 a model presenting a degenerate cycle is given.

2. Preliminaries

The switching manifold $\Sigma = \{p \in \mathbb{R}^2;\ h(p) = 0\}$ is the hypersurface boundary between the regions $\Sigma^+ = \{p \in \mathbb{R}^2;\ h(p) > 0\}$ and $\Sigma^- = \{p \in \mathbb{R}^2;\ h(p) < 0\}$. It is partitioned into the following regions depending on the directions of X and Y:

- the crossing region, where $\Sigma^c = \{p \in \Sigma;\ Xh.Yh(p) > 0\}$;
- the sliding region, where $\Sigma^s = \{p \in \Sigma;\ Xh(p) < 0 \text{ and } Yh(p) > 0\}$;
- the escaping region, where $\Sigma^e = \{p \in \Sigma;\ Xh(p) > 0 \text{ and } Yh(p) < 0\}$.

For all $X \in \chi^r$, the scalar $Xh(p) = \langle X, \nabla h \rangle(p)$ is the Lie derivative of h with respect to X at p. The regions $\Sigma^c, \Sigma^s, \Sigma^e$, are open in Σ and their complement in Σ is the set of all points satisfying $Xh(p).Yh(p) = 0$, called boundary singular (if

p is a singular point of X or Y) or tangency points (p is neither a singular point of X nor Y). A smooth vector field X is transversal to Σ at $p \in \Sigma$ if $Xf(p) \neq 0$.

Taking $Z = (X, Y) \in \Omega^r$, if $p \in \Sigma^+$ (resp. $p \in \Sigma^-$) then the trajectory of Z through p is the local trajectory of X (resp. Y) through this point. If $p \in \Sigma^c$ the trajectory of Z through p is the concatenation of the respective trajectories of X in Σ^+ and of Y in Σ^-. If $p \in \Sigma^s \cup \Sigma^e$ then the trajectory of Z through this point is the trajectory of the sliding vector field Z^s through p. The vector field Z^s is defined as the unique convex combination of X and Y that is tangent to Σ, given by

$$(2) \qquad Z^s(p) = \frac{1}{Yf(p) - Xf(p)} \left(Yf(p)X(p) - Xf(p)Y(p) \right),$$

for $p \in \Sigma^s \cup \Sigma^e$. It is useful to define also the normalized sliding vector field $Z_N^s(p) = Yf(p)X(p) - Xf(p)Y(p)$.

The singular points of Z^s in $\Sigma^s \cup \Sigma^e$ are called *pseudo-singular* points. Those singular points of X (resp. Y) that lie on Σ^+ (resp. Σ^-) are called *real singular* points, and those singular points of X (resp. Y) that lie on Σ^- (resp. Σ^+) are called *virtual singular* points. The singularities of $Z = (X, Y)$ are: real singular points, boundary singular points pseudo-equilibria points and tangency points. The points that are not singularities are called regular points.

Definition 1. *A smooth vector field X has a fold singularity or a quadratic tangency at $p \in \Sigma$ if $Xh(p) = 0$ and $X^2h(p) \neq 0$, with $X^2h(p) = \langle X, \nabla Xh \rangle(p)$. A nonsmooth vector field $Z = (X, Y)$ has a fold singularity at $p \in \Sigma$ if p is a fold for X or Y. A fold point p for X (resp. Y) is visible if $X^2h(p) > 0$ (resp. $Y^2h(p) < 0$) and invisible if $X^2h(p) < 0$ (resp. $Y^2h(p) > 0$). If p is a fold for X and a regular point for Y (or vice-versa) then p is a fold-regular point for Z.*

Definition 2. *A nonsmooth vector field Z has a saddle-regular point at $p \in \Sigma$ if p is a saddle point for X (resp. Y), and Y (resp. X) is transversal to Σ at p.*

Denote a trajectory of $\dot{x} = Z$ by $\varphi_Z(t, q)$ where $\varphi_Z(0, q) = q$. Taking $q \in \Sigma^+ \cup \Sigma^-$, a point $p \in \Sigma$, p is said to be a departing point (resp. arriving point) of $\varphi_Z(t, q)$ if there exists $t_0 < 0$ (resp. $t_0 > 0$) such that $\lim_{t \to t_0^+} \varphi_Z(t, q) = p$ (resp. $\lim_{t \to t_0^-} \varphi_Z(t, q) = p$). With these definitions if $p \in \Sigma^c$, then it is a departing point (resp. arriving point) of $\varphi_X(t, q)$ for any $q \in \gamma^+(p)$ (resp. $q \in \gamma^-(p)$), where

$$\gamma^+(p) = \{\varphi_Z(t, p); t \in I \cap \{t \geq 0\}\}, \quad \gamma^-(p) = \{\varphi_Z(t, p); t \in I \cap \{t \leq 0\}\},$$

and $I \subset \mathbb{R}$ is the interval for which $\varphi_Z(\cdot, p)$ is defined. To distinguish between the main types of orbits and cycles we have the following.

Definition 3. *A continuous closed curve Γ is said to be a cycle of the vector field Z if it is composed by a finite union of segments of regular orbits and singularities, $\gamma_1, \gamma_2, \ldots, \gamma_n$, of Z. There are different types of cycle Γ:*

- *Γ is a simple cycle if none of the γ_i's are singular points and the set $\gamma_i \cap \Sigma$ is either empty or composed only by points of Σ^c, $\forall i = 1, \ldots, n$. If such a cycle is isolated in the set of all simple cycles of Z then it is called a limit cycle. See figure 2(a);*
- *Γ is a regular polycycle if either, for all $i = 1, \ldots, n$, the set $\gamma_i \cap \Sigma$ is empty and at least one of $\gamma_i's$ is a singular point or, for some $i = 1, \ldots, n$, $\gamma_i \cap \Sigma$*

is nonempty but only contains points of $\overline{\Sigma^c}$ that are not tangent points of Z. See figures 2(b) and 2(c);

- Γ is a *sliding cycle* if there exists $i \in \{1, 2, \ldots, n\}$ such that γ_i is a segment of sliding orbit and, for any two consecutive curves, the departing or arriving points in Σ are not the same. See figure 2(d);
- Γ is a *pseudo-cycle* if for some $i \in \{1, 2, \ldots, n\}$, the arriving points (or departing points) of γ_i and γ_{i+1} are the same. See figures 2(e) and 2(f).
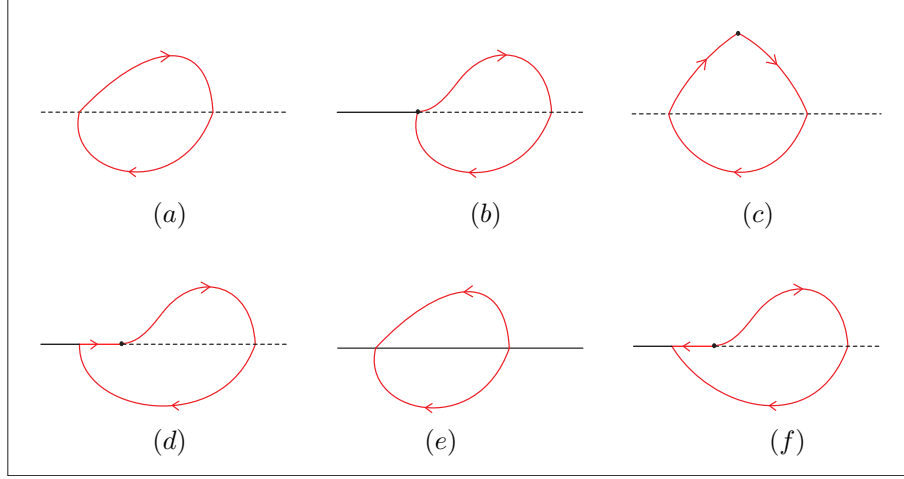
FIGURE 2. Illustration of different types of cycles: (a) simple cycle; (b), (c) regular polycycles; (d) sliding cycle; (e) pseudo-cycle and (f) sliding pseudo-cycle.

Definition 4. *(See* [4]*) An unstable (resp. a stable) separatrix is either:*

- *a regular orbit Γ that is the unstable (resp. stable) invariant manifold of a saddle point $p \in \overline{\Sigma^+}$ of X or $p \in \overline{\Sigma^-}$ of Y, denoted by $W^u(p)$ (resp. $W^s(p)$); or*
- *a regular orbit that has a distinguished singularity $p \in \Sigma$ as departing (resp. arriving) point. It is denoted by $W^u_\pm(p)$ (resp. $W^s_\pm(p)$) and $\pm$ means that it leaves (resp. arrives) from $\Sigma^\pm$.*

Where necessary, we use the notation $W^{s,u}_\pm(X, p)$ to indicate which vector field is being considered. If a separatrix is at the same time unstable and stable then it is a *separatrix connection*. A orbit Γ that connects two singularities, p and q, of Z, will be called either a *homoclinic connection* if $p = q$ or a *heteroclinic connection* if $p \neq q$.

Definition 5. *A hyperbolic pseudo-equilibrium point p is said to be a*

- *pseudonode if $p \in \Sigma^s$ (resp. $p \in \Sigma^e$) and it is an attractor (resp. a repeller) for the sliding vector field;*
- *pseudosaddle if $p \in \Sigma^s$ (resp. $p \in \Sigma^e$) and it is a repeller (resp. an attractor) for the sliding vector field.*

3. Degenerate cycle passing through a saddle-regular point

We start by establishing the necessary generic conditions to obtain a degenerate cycle with lowest possible codimension. Consider a nonsmooth vector field $Z_0 = (X_0, Y_0) \in \Omega^r$ satisfying the following conditions:

- $BS(1)$: X_0 has a hyperbolic saddle at $S_{X_0} \in \Sigma$ and the invariant manifolds of X_0 at the saddle point S_{X_0}, $W^u(X_0, S_{X_0})$ and $W^s(X_0, S_{X_0})$, are transversal to Σ at S_{X_0};
- $BS(2)$: Y_0 is transversal to Σ, $W^u(X_0, S_{X_0})$, and $W^s(X_0, S_{X_0})$ at S_{X_0};
- $BS(3)$: the normalized sliding vector field has S_{X_0} as a hyperbolic singularity, by taking x as a local chart on Σ at S_{X_0}, $Z_N^s(x) = \mu x + O(x^2)$ with $\mu \neq 0$;
- $BSC(1)$: the unstable manifold of the saddle that lies in Σ^+, $W_+^u(X_0, S_{X_0})$, is transversal to Σ at $P_{X_0} \neq S_{X_0}$. We have $\varphi_{X_0}(t, P_{X_0}) \in \Sigma^+$ for all $t < 0$;
- $BSC(2)$: Y_0 is transversal to Σ at P_{X_0} and there exists $t_0 > 0$ such that $\varphi_{Y_0}(t_0, P_{X_0}) = S_{X_0}$ and $\varphi_{Y_0}(t, P_{X_0}) \in \Sigma^-$ for all $0 < t < t_0$.

Remark 1. *Under the conditions above, the saddle-regular point is on the boundary of a crossing region and an escaping or sliding region, i.e, $S_{X_0} \in \partial\Sigma^e \cup \partial\Sigma^c$ or $S_{X_0} \in \partial\Sigma^s \cup \partial\Sigma^c$.*

There are two different topological types of cycles satisfying $BS(1)$-$BS(3)$ and $BSC(1)$-$BSC(2)$, see Figure 3.
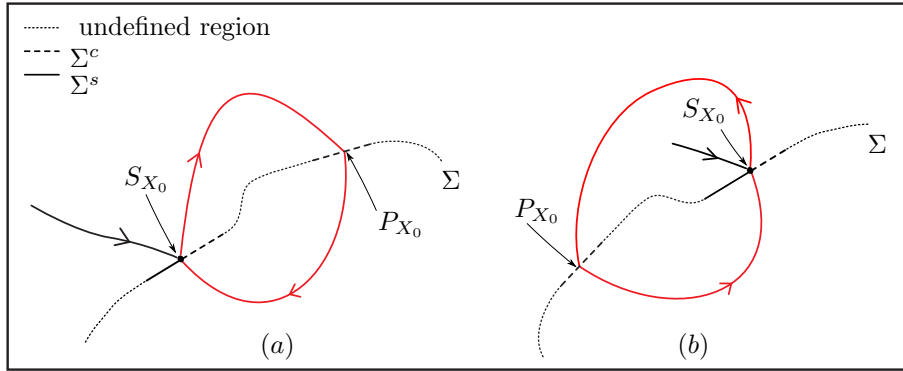

FIGURE 3. A degenerate cycle passing through a saddle-regular point: (a) $W_+^s(X_0, S_{X_0})$ contained in the unbounded region and (b) $W_+^s(X_0, S_{X_0})$ contained in the bounded region.

Despite the fact that both cases shown in Figure 3 are topologically distinct, their analysis is similar, so we focus on case (a). Whenever we refer to a degenerate cycle through a saddle point, we refer to a cycle as given in case (a) of Figure 3.

To study the unfolding of the cycle, we look carefully at the local saddle-regular bifurcation, after that we perform a study on the first return map defined near the cycle.

3.1. **Bifurcation of a saddle-regular singularity.** The simplest case is the codimension 1 bifurcation studied in [4, 1], which we review briefly here for completeness. Consider a nonsmooth vector field $Z_0 = (X_0, Y_0) \in \Omega^r$ satisfying conditions $BS(1)$-$BS(3)$. To study bifurcations of Z_0 near S_{X_0}, the following result from [5]

is important, describing bifurcations of a hyperbolic saddle point on the boundary Σ of the manifold with boundary $\overline{\Sigma^+} = \Sigma \cup \Sigma^+$.

Lemma 1. *Let $p \in \Sigma$ be a hyperbolic saddle point of $X_0|_{\overline{\Sigma^+}}$, where $X_0 \in \chi^r$. Then there exist neighborhoods B_0 of p in $\mathbb{R}^2$ and $\mathcal{V}_0$ of X_0 in χ^r, and a C^r map $\beta : \mathcal{V}_0 \to \mathbb{R}$, such that:*

- (a) *$\beta(X) = 0$ if and only if X has a unique equilibrium $p_X \in \Sigma \cap B_0$ that is a hyperbolic saddle point;*
- (b) *if $\beta(X) > 0$, X has a unique equilibrium $p_X \in B_0 \cap int(\Sigma^+)$ that is a hyperbolic saddle point;*
- (c) *if $\beta(X) < 0$, X has no equilibria in $B_0 \cap \overline{\Sigma^+}$.*

Since Y_0 is transversal to Σ at S_{X_0}, there exist neighborhoods B_1, of S_{X_0} in Σ, and $\mathcal{V}_1$, of Y_0 in χ^r, such that for any $Y \in \mathcal{V}_1$ and $p \in B_1$, Y is transversal to Σ at p. Taking B_0 as given in Lemma 1 there is no loss of generality in supposing $B_0 \cap \Sigma = B_1$ and then restrict ourselves to the neighborhood $\mathcal{V}_{Z_0} = \mathcal{V}_0 \times \mathcal{V}_1$ of Z_0 in Ω^r.

If $\beta(X) \neq 0$, for $X \in \mathcal{V}_0$, there exists a fold point of X in B_1. The fold point is located between the points where the invariant manifolds of the saddle cross Σ. The map $s : \mathcal{V}_0 \to \Sigma$ that associates each $X \in \mathcal{V}_0$ to a tangent point $F_X \in \Sigma$ is of class C^r, F_X is visible fold point if $\beta(X) < 0$, F_X is a hyperbolic saddle point if $\beta(X) = 0$, F_X is an invisible point if $\beta(X) > 0$.

Each $Z = (X, Y) \in \mathcal{V}_{Z_0}$ can be associated with two curves, T_X and PE_Z, defined as follows:

- (i) $T_X = \{p \in \mathbb{R}^2; Xh(p) = 0\}$ is the curve formed by all points in $\mathbb{R}^2$ where X is parallel to Σ. Therefore, the intersection of T_X with Σ gives the fold point F_X.
- (ii) $PE_Z = \{p \in \mathbb{R}^2; X(p) \text{ is parallel to } Y(p)\}$ is the curve composed by those points in $\mathbb{R}^2$ for which X and Y are parallel. So, when the intersection of PE_Z with Σ belongs to $\Sigma^s \cup \Sigma^e$ it coincides with the pseudo-equilibrium point.

The maps $X \mapsto T_X$ and $Z \mapsto PE_Z$ are of class C^r. It follows from conditions $BS(1)$-$BS(3)$ that the curves T_{X_0}, PE_{Z_0}, $W^u(X_0, S_{X_0})$ and $W^s(X_0, S_{X_0})$ have empty intersection in B_0 up to the saddle point S_{X_0}. In fact, all these curves contain the singular point S_{X_0}. Condition $BS(2)$ guarantees that PE_{Z_0}, $W^u(X_0, S_{X_0})$ and $W^s(X_0, S_{X_0})$ do not coincide in B_0 up to the saddle point. Condition $BS(3)$ also ensures that T_{X_0} and PE_{Z_0} are different in B_0 except at S_{X_0}.

The continuous dependence of the curves T_{X_0}, PE_{Z_0}, $W^u(X_0, S_{X_0})$ and $W^s(X_0, S_{X_0})$, on the vector field ensures that $\mathcal{V}_{Z_0}$ can be taken in such a way that the relative position of these curves do not change for all $Z \in \mathcal{V}_{Z_0}$. The curve T_{X_0} is located between $W^s_+(X_0, S_{X_0})$ and $W^u_+(X_0, S_{X_0})$, see Figure 4.

Since $S_{X_0} \in \partial \Sigma^s \cup \partial \Sigma^c$ there are three different cases to consider depending on the position of PE_{Z_0} in relation to T_{X_0}, $W^s_+(X_0, S_{X_0})$, and $W^u_+(X_0, S_{X_0})$, see 4. These cases are named BS_1, BS_2 and BS_3 as in [1].
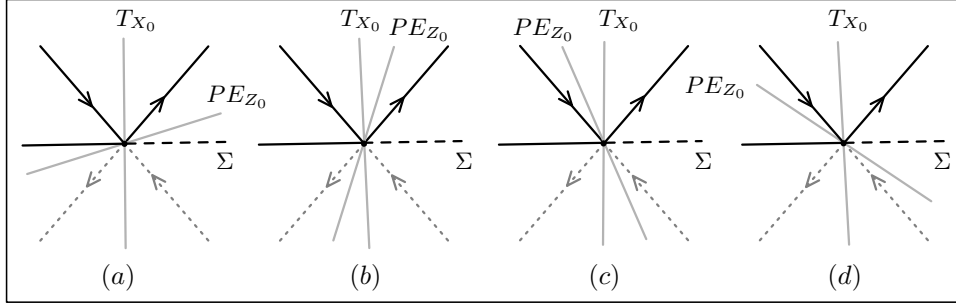
FIGURE 4. Relative position of the curves T_{X_0}, PE_{Z_0}, $W_+^s(X_0, S_{X_0})$, and $W_+^u(X_0, S_{X_0})$. (a) corresponds to case BS_1, (b) corresponds to case BS_2 and $(c) - (d)$ both correspond to case BS_3.

To understand the difference between BS_1, BS_2 and BS_3, for $Z = (X, Y) \in \mathcal{V}_{Z_0}$ let $\beta = \beta(X)$ be given by Lemma 1. Then S_X is a real saddle if $\beta > 0$, a boundary saddle if $\beta = 0$, or a virtual saddle if $\beta < 0$.

1. Case BS_1: this happens when $W_+^u(S_{X_0}, X_0)$ is between T_{X_0} and PE_{Z_0} in Σ^+, see Figure 4(a). If the saddle is virtual $(\beta < 0)$, the saddle-regular point turns into a visible fold-regular point and there is no pseudo-equilibrium. The fold-regular point is an attractor for the sliding vector field. Also, when the saddle is real $(\beta > 0)$, an invisible fold-regular point emerges and there exists an attracting pseudo-node. The point in Σ^s where the unstable manifold of the saddle crosses Σ is located between the pseudo-equilibrium and the fold-regular point, see Figure 5.
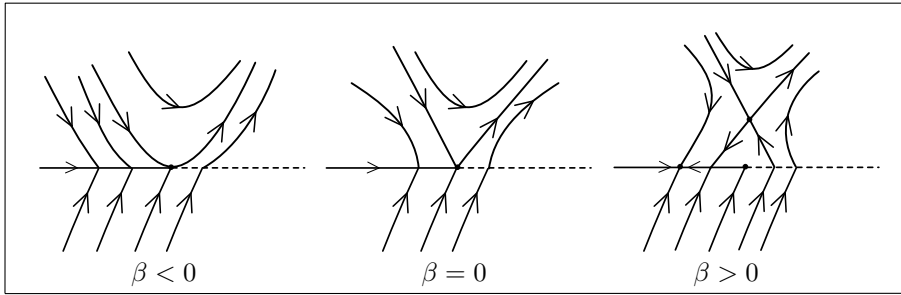

FIGURE 5. Bifurcation of a saddle-regular point: case BS_1.

2. Case BS_2: this case happens when PE_{Z_0} is between T_{X_0} and $W_+^u(S_{X_0}, X_0)$ in Σ^+, see Figure 4(b). There is a visible fold-regular point and there is no pseudo-equilibrium when the saddle is virtual $(\beta < 0)$. The fold-regular point is an attractor for the sliding vector field. When the saddle is real $(\beta > 0)$, an invisible fold-regular point and an attracting pseudo-node coexist. The pseudo-equilibrium is located between the point (in Σ^s) where the unstable manifold of the saddle meets Σ and the fold-regular point. See Figure 6.
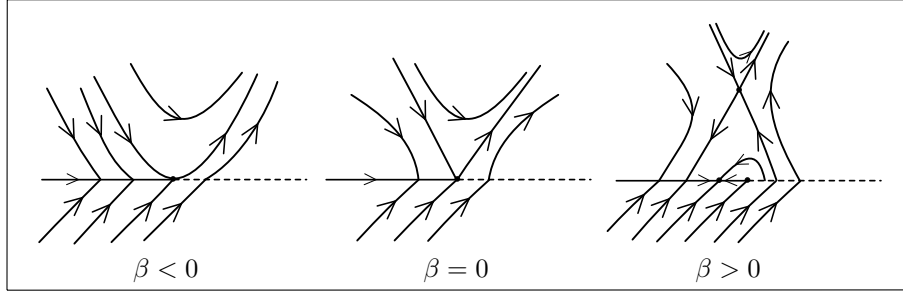
FIGURE 6. Bifurcation of a saddle-regular point: case BS_2.

3. Case BS_3: this case happens when T_{X_0} is between $W_+^u(S_{X_0}, X_0)$ and PE_{Z_0} in Σ^+, see Figures 4(c)-(d). When the saddle is virtual ($\beta < 0$), a visible fold-point coexists with a pseudo-saddle. There exists no pseudo-equilibrium when the saddle is real ($\beta > 0$). In this case, the saddle-regular point turns into an invisible fold-regular point that is a repeller for the sliding vector field. See Figure 7.
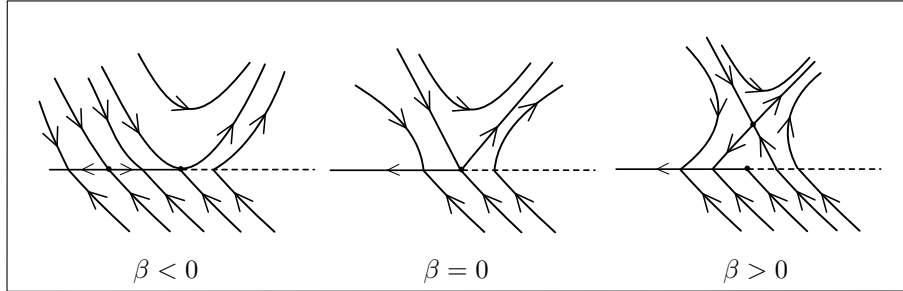

FIGURE 7. Bifurcation of a saddle-regular point: case BS_3.

3.2. **Structure of the first return map.** Let Γ_0 be the degenerate cycle of Z_0. We show that $\mathcal{V}_{Z_0}$ can be chosen in such a way that, for each $Z \in \mathcal{V}_{Z_0}$, a first return map is defined in a half-open interval, near the cycle Γ_0.

Proposition 1. *Let Z_0 be a nonsmooth vector field satisfying conditions $BS(1)$-$BS(3)$ and $BSC(1)$-$BSC(2)$. In addition, suppose S_{X_0} is located at the origin. Then there exists a neighborhood $\mathcal{V}_{Z_0}$ of Z_0 in Ω^r such that, for all $Z \in \mathcal{V}_{Z_0}$, there is a well defined first return map in a half-open interval $[a_Z, a_Z + \delta_Z)$ with $\delta_Z > 0$ and $a_Z \approx 0$. The first return map of Z can be written as*

$$\pi_Z(x) = \rho_3 \circ \rho_2 \circ \rho_1(x),$$

where ρ_2 and ρ_3 are orientation reversing diffeomorphisms and ρ_1 is a transition map near a saddle or a fold point.

Proof. We have already determined a neighborhood $\mathcal{V}_{Z_0} = \mathcal{V}_0 \times \mathcal{V}_1$ where, for all $Z = (X, Y) \in \mathcal{V}_{Z_0}$, Lemma 1 holds for X and transversality conditions hold for Y in $B_1 = B_0 \cap \Sigma$. The claimed existence follows directly by means of continuous dependence results and properties of transversal sets.

Now we determine a_Z for each $Z \in \mathcal{V}_{Z_0}$. When the saddle of X is not in Σ, there are at least three different points in which the invariant manifolds $W^{u,s}(X, S_X)$ meet Σ. Denote these points by P_X^i, $i = 1, 2, 3$, where $P_X^1, P_X^2 \in B_1$ and $P_X^3 \in I_1$ (I_1 is a neighborhood of P_{X_0} in Σ). Assume $P_X^1, P_X^3 \in W^u(S_X, X) \cap \Sigma$ and $P_X^2 \in W^s(S_X, X) \cap \Sigma$. We keep this notation if the saddle is on Σ, in this case $P_X^1 = P_X^2 = S_X$. By taking x as a local chart for Σ near 0 (with $x < 0$ corresponding to sliding region and $x > 0$ corresponding to crossing region) and by denoting $P_X^i = x_i$, $i = 1, 2$, we have $x_1 \leq x_2$. If $S_X \notin \Sigma$ then there exists a tangency point $F_X \in B_1$, also $S_X = F_X$ when the saddle is on the boundary. Considering the previous chart for Σ, denote $F_X = x_f$, then $x_1 \leq x_f \leq x_2$, see Figure 8. Observe that $\lim_{Z \to Z_0} x_i = 0$ for $i = 1, 2, f$. For $Z \in \mathcal{V}_{Z_0}$ let a_Z be defined as $a_Z = x_f$ if $\beta(X) < 0$, $a_Z = x_1 = x_2$ if $\beta(X) = 0$, or $a_Z = x_2$ if $\beta(X) > 0$. Thus, by choosing $\delta_Z > 0$ small enough the existence of the first return map in $[a_Z, a_Z + \delta_Z]$ is ensured by continuity.

To study the structure of this first return map for $Z \in \mathcal{V}_{Z_0}$, we analyze it near the saddle point. Without loss of generality, suppose that Σ is transversal to the y axis at the origin. Consider a sufficiently small $\varepsilon > 0$ and let σ denote a section transversal to the flow of X, for $x > 0$, through the point $(0, \varepsilon)$. There are three options for the position of S_X in relation to Σ, in each case the first return map is analysed differently. As above, consider $\beta = \beta(X)$ then:

- if $\beta < 0$, S_X is virtual, then the first return map is limited by the visible fold point, F_X. So we have a transition map, ρ_1, from Σ to σ near a fold point. See Figure 8(a);
- if $\beta = 0$, $S_X \in \Sigma$, then we have a transition map, ρ_1, from Σ to σ near a boundary saddle point. See Figure 8(b);
- if $\beta > 0$, S_X is real, then the limit point of the first return map is the point P_X^2 where the stable manifold $W_+^s(X, S_X)$ intersects Σ near 0. There is a transition map, ρ_1, from Σ to σ, near a real saddle point. See Figure 8(c).

After crossing through σ, the orbits will cross Σ near P_X^3. Since σ is a transversal section, the transition from σ to Σ is performed by means of a diffeomorphism ρ_2. The flow of Y makes the transition from Σ (near P_X^3) to Σ (near 0), then the transversal conditions satisfied by Y give another diffeomorphism, ρ_3, performing this transition. The diffeomorphisms ρ_2 and ρ_3 are orientation reversing, so we can write $\pi_Z(x) = \rho_3 \circ \rho_2 \circ \rho_1(x)$ for $x \in [a_Z, a_Z + \delta_Z]$. $\qquad \square$
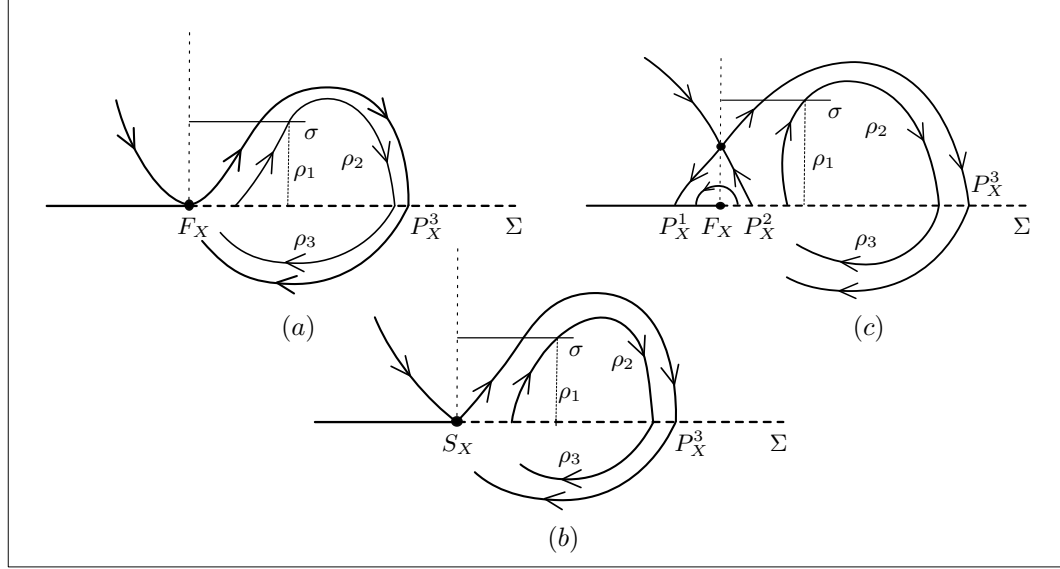
FIGURE 8. Illustration of the first return map with transversal section τ: (a) $\beta < 0$, (b) $\beta = 0$ and (c) $\beta > 0$.

Since ρ_2 and ρ_3 given in Proposition 1 are diffeomorphisms, the difficult part in understanding the first return map π_Z is the structure of ρ_1. From now on we assume $Z_0 = (X_0, Y_0) \in \Omega^\infty$, since high differentiability classes are required. We restrict the analysis to nonresonant saddles, meaning we consider $Z = (X, Y) \in \mathcal{V}_{Z_0}$ such that the hyperbolicity ratio of S_X, r, is an irrational number, $(r = -\lambda_2/\lambda_1$ where $\lambda_2 < 0 < \lambda_1$ are the eigenvalues of $DX(S_X)$). The point S_X is assumed to lie at the origin.

According to [6], for each l, X is C^l-conjugated, around S_X, to the normal form

$$(3) \qquad \tilde{X}(x, y) = -rx\frac{\partial}{\partial x} + y\frac{\partial}{\partial y}.$$

Let us assume that $\Sigma = h_k^{-1}(0)$ where $h_k(x, y) = y - x + k$. Then Σ intersects the axes at $(0, -k)$ and $(k, 0)$, implying that if $k > 0$ then the saddle is real, if $k = 0$ then the saddle is on the boundary, and if $k < 0$ the saddle is virtual.

Denote the flow of $\tilde{X}$ by $\varphi_{\tilde{X}}(t, x, y) = (\varphi_1(t, x, y), \varphi_2(t, x, y))^T$ and $\tilde{\sigma}$ be the transversal section of $\tilde{X}$ associated with the transversal section σ of X. Without loss of generality, assume $\tilde{\sigma} \subset \{(x, 1) \in \mathbb{R}^2; x > 0\}$. In this case, the transition time from Σ to $\tilde{\sigma}$ is easily calculated and it is given by $t_1(x) = -\ln(x - k)$ for each $(x, x - k) \in \Sigma$. Therefore, the transition map $\tilde{\rho}$, from Σ to $\tilde{\sigma}$, is given by $\tilde{\rho}(x) = \varphi_2(t_1(x), x, x - k) = e^{-rt_1(x)}x = x(x - k)^r = k(x - k)^r + (x - k)^{r+1}$. Since X and $\tilde{X}$ are conjugated, there must exist diffeomorphisms ϕ and ψ, defined in a neighborhood of the origin, such that $\rho = \phi \circ \tilde{\rho} \circ \psi$ and $\psi(0) = \phi(0) = 0$. We can also assume that $\tilde{a} = \psi(a_Z)$ is equivalent to a_Z, i.e., the transition map $\tilde{\rho}$ of $\tilde{X}$ is defined in $[\tilde{a}, \tilde{a} + \tilde{\delta})$, $\tilde{\delta} > 0$. Then:

- if $k < 0$, then $k < \tilde{a} = \dfrac{k}{1 + r} < 0$. This means that $F_X = \left(\dfrac{k}{1 + r}, \dfrac{-kr}{1 + r}\right)$; see Figure 9(a)

- if $k \geq 0$, then $\tilde{a} = k$. This means $P_2 = (k, 0)$ for $k > 0$ and $S_X = (0,0)$ for $k = 0$; see Figures $9(b)$ and $9(c)$.
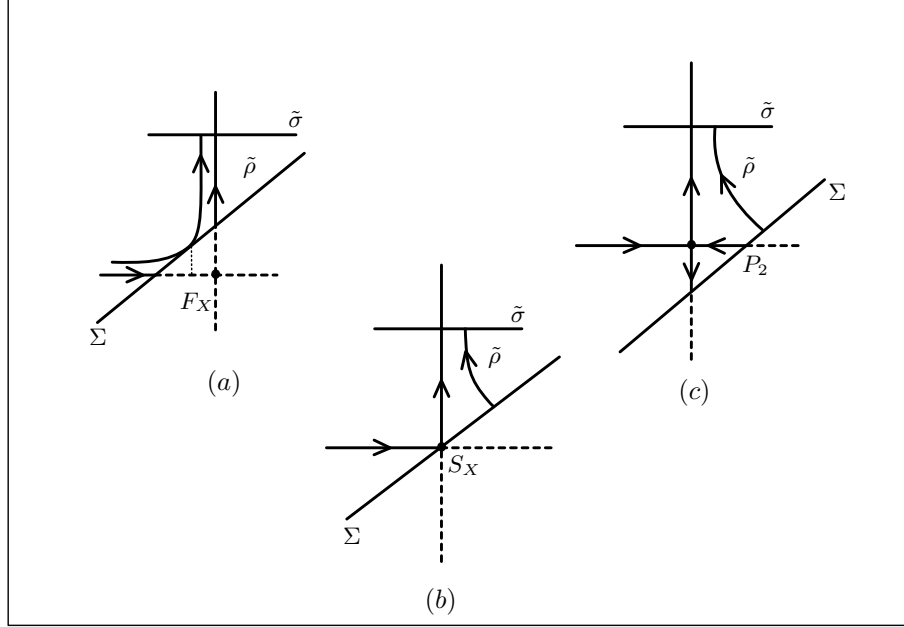

FIGURE 9. Illustration of the transition map $\tilde{\rho}$, from Σ to $\tilde{\sigma}$: (a) $k < 0$, (b) $k = 0$ and (c) $k > 0$.

Proposition 2. *Consider $Z = (X, Y) \in \mathcal{V}_{Z_0}$, let $r \notin \mathbb{Q}$ be the hyperbolicity ratio of S_X and $s = [r]$. Let $\beta = \beta(X)$ be defined in Lemma 1 and π_Z defined in Proposition 1. Then:*

(i) $\dfrac{d}{dx} \pi_Z(a_Z) = 0$ *and* $\dfrac{d^2}{dx^2} \pi_Z(a_Z) > 0$ *if $\beta < 0$;*

(ii) $\displaystyle\lim_{x \to a_Z^+} \dfrac{d}{dx} \pi_Z(x) = \cdots = \lim_{x \to a_Z^+} \dfrac{d^{s+1}}{dx^{s+1}} \pi_Z(x) = 0$ *and* $\displaystyle\lim_{x \to a_Z^+} \dfrac{d^{s+2}}{dx^{s+2}} \pi_Z(x) = +\infty$ *if $\beta = 0$ and $r > 1$;*

(iii) $\displaystyle\lim_{x \to a_Z^+} \dfrac{d}{dx} \pi_Z(x) = +\infty$ *if $\beta \geq 0$ and $r < 1$;*

(iv) $\displaystyle\lim_{x \to a_Z^+} \dfrac{d}{dx} \pi_Z(x) = \cdots = \lim_{x \to a_Z^+} \dfrac{d^s}{dx^s} \pi_Z(x) = 0$ *and* $\displaystyle\lim_{x \to a_Z^+} \dfrac{d^{s+1}}{dx^{s+1}} \pi_Z(x) = +\infty$ *if $\beta > 0$ and $r > 1$.*

Proof. From Proposition 1 we know $\pi_Z = \rho_3 \circ \rho_2 \circ \rho_1$. Observe that ρ_2 and ρ_3 are orientation reversing diffeomorphisms of class C^∞, and that $\rho_1 = \phi \circ \tilde{\rho} \circ \psi$ where ϕ and ψ are orientation preserving diffeomorphisms of class $\mathcal{C}^l$, $l > s + 2$. Define $\Phi = \rho_3 \circ \rho_2 \circ \phi$, then $\pi_Z = \Phi \circ \tilde{\rho} \circ \psi$, where Φ and ψ are orientation preserving diffeomorphisms of class $\mathcal{C}^l$ with $l > s + 2$. By definition, $\tilde{a} = \psi(a_Z)$. Let I_0 be a neighborhood of a_Z where $\pi_Z = \Phi \circ \tilde{\rho} \circ \psi(x)$ is well defined for $x \in I_0$. Then the derivatives of order $1 \leq i \leq s+2$ of Φ and ψ are limited in I_0, and $\tilde{\rho}$ is differentiable in $(\tilde{a}, \tilde{a} + \tilde{\delta})$ for $\tilde{\delta} > 0$ sufficiently small.

Now

$$\frac{d}{dx}\pi_Z(x) = \frac{d}{dx}\Phi(\tilde{\rho}(\psi(x)))\frac{d}{dx}\tilde{\rho}(\psi(x))\frac{d}{dx}\psi(x).$$

Thus, for each $1 < i \leq s + 2$, the result follow by means of the chain and product rules for derivatives and from the fact that $\psi(x) \to \tilde{a}^+$ when $x \to a_Z^+$. $\qquad\square$

Proposition 3. *Consider $Z = (X,Y) \in \mathcal{V}_{Z_0}$ and suppose that $r \notin \mathbb{Q}$ is the hyperbolicity ratio of S_X. Then the following statements hold:*

(i) *If $\pi_Z(a_Z) > a_Z$ and either $r > 1$ or $r < 1$ and $\beta(Z) \leq 0$, then there exists an attractor fixed point of π_Z, $x_0 \in (a_Z, \delta_Z)$, which corresponds to an attracting limit cycle of Z.*

(ii) *If $\pi_Z(a_Z) = a_Z$ and either $r > 1$ or $r < 1$ and $\beta(Z) \leq 0$ then, a_Z is an attractor for π_Z. So, there exists an attracting degenerate cycle for Z through a fold-regular point if $\beta(Z) < 0$, a saddle-regular point if $\beta(Z) = 0$, or a real saddle if $\beta(Z) > 0$.*

(iii) *If $\pi_Z(a_Z) < a_Z$, $r < 1$, and $\beta(Z) > 0$, then there exists a repelling fixed point of π_Z, $x_0 \in (a_Z, \delta_Z)$, which corresponds to a repelling limit cycle of Z.*
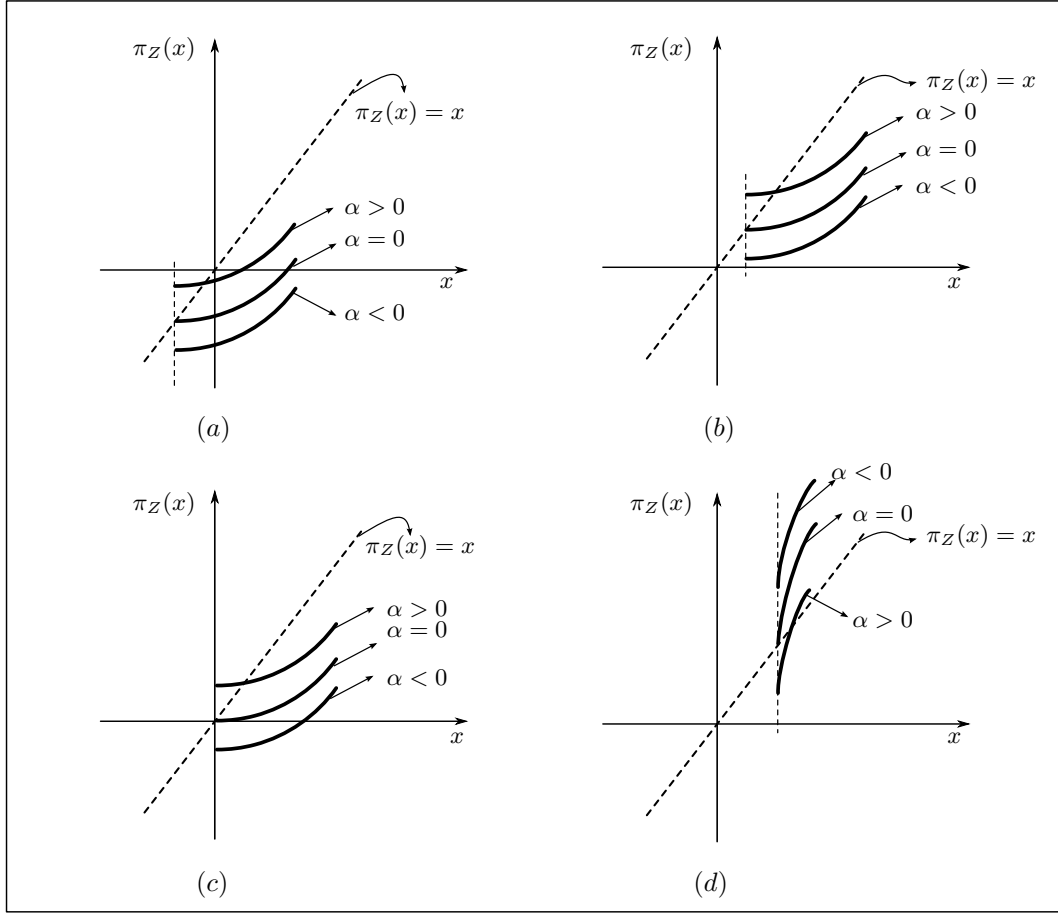
FIGURE 10. Illustration of the graph of the first return map $\pi_Z(x)$ for $x \in [a_Z, a_Z + \delta_Z)$ where $\alpha = \pi_Z(a_Z) - a_Z$. (a) $\beta(Z) < 0$, (b) $\beta(Z) > 0$ and $r > 1$, (c) $\beta(Z) = 0$, and (d) $\beta(Z) > 0$ and $r < 1$.

Proof. From the definition of $\tilde{\rho}(x)$ it is increasing in $[\tilde{a}, \tilde{a} + \tilde{\delta})$. Also, from the proof of Proposition 2 we have $\pi_Z = \Phi \circ \tilde{\rho} \circ \psi$ where Φ and ψ are orientation preserving diffeomorphisms, or, in other words, increasing maps since the first derivative of these maps are positive.

Also from Proposition 2, if $r > 1$, the tangent vector of the graph of $\pi_Z(x)$ tends to be horizontal when $x \to a_Z^+$. Analogously, if $r < 1$, the tangent vector of the graph of $\pi_Z(x)$ tends to be vertical when $x \to a_Z^+$. See Figure 10.

So if $\pi_Z(a_Z) = a_Z$ and $r > 1$, taking the smallest possible δ_Z if necessary, a_Z is the unique fixed point of π_Z in $[a_Z, a_Z + \delta_Z)$ and $\pi_Z(x) < x$ for all $x \in (a_Z, a_Z + \delta_Z)$. Therefore a_Z is an attracting fixed point of π_Z that corresponds to a degenerate cycle Z. The definition of a_Z gives the different types of cycles as listed in item (ii). Analogously, if $\pi_Z(a_Z) = a_Z$, $r < 1$ and $\beta(Z) > 0$, a_Z is the unique fixed point of p_Z in $[a_Z, a_Z + \delta_Z)$ and $\pi_Z(x) > x$ for all $x \in (a_Z, a_Z + \delta_Z)$. Then a_Z is a repeller for π_Z that corresponds to a repelling degenerate cycle of Z through a real saddle point. This proves item (ii).

If $\pi_Z(a_Z) > a_Z$ and either $r > 1$ or $r < 1$ and $\beta(Z) \leq 0$, the analysis is similar to the case in item (ii), the only difference is that the fixed point will change. Since in these cases the tangent vector of the graph of π_Z tends to be horizontal at a_Z, for Z sufficiently near Z_0 (taking the smallest $\mathcal{V}_{Z_0}$ if necessary), the graph of π_Z intersects the graph of the identity map at a point $x_0 \in (a_Z, a_Z + \delta_Z)$. Also, $\pi_Z(x) > x$ for all $x \in [a_Z, x_0)$ and $\pi_Z(x) < x$ for all $x \in (x_0, a_Z + \delta_Z)$. This proves item (i).

To prove item (iii) it is enough to observe that, since the tangent vector of the graph of π_Z tends to be vertical at a_Z, we obtain that the graph of π_Z will cross the graph of the identity map at a point $x_0 \in (a_Z, a_Z + \delta_Z)$. Also, $\pi_Z(x) < x$ for all $x \in [a_Z, x_0)$ and $\pi_Z(x) > x$ for all $x \in (x_0, a_Z + \delta_Z)$. This proves item (iii). $\square$

4. Main Results and Bifurcation Diagrams

In this section, we focus on a discussion of all phenomena of codimension 1 that appear in the characterization of the bifurcation diagram in question. There exist two independent ways of breaking the structure of the degenerate cycle of Z_0: to translate of the saddle or to destroy the homoclinic connection. More specifically, there exist two bifurcation parameters to consider, β and α, given as following:

- β is a C^r-map that determines if the saddle of X is real, on the boundary, or virtual. This map was determined in Lemma 1, and now it is naturally extended to $\mathcal{V}_{Z_0}$,

$$\beta: \begin{array}{ccc} \mathcal{V}(Z_0) & \rightarrow & \mathbb{R} \\ (X, Y) & \mapsto & \beta(X) \end{array}.$$

- α is a C^r-map that determines whether or not the first return map has a fixed point,

$$\alpha: \begin{array}{ccc} \mathcal{V}(Z_0) & \rightarrow & \mathbb{R} \\ Z & \mapsto & \pi_Z(a_Z) - a_Z \end{array}.$$

Despite the fact that a_Z was defined in terms of $\text{Sgn}(\beta)$, the quantity $\alpha(Z)$ is an intrinsic feature of Z.

Define $\mathcal{V}_0 = \{Z = (X, Y) \in \mathcal{V}_{Z_0}; S_X$ has irrational hyperbolicity ratio$\}$. From now on we only consider vector fields in $\mathcal{V}_0$ and describe the bifurcations of Z_0 in $\mathcal{V}_0$. To do so, consider a family of nonsmooth vector fields $Z_{\alpha,\beta}$ of vector fields in $\mathcal{V}_0$, $(\alpha, \beta) \in \mathcal{B}_0 \subset \mathbb{R}^2$, such that $\mathcal{B}_0$ is an open neighborhood of $0 \in \mathbb{R}^2$, $Z_{0,0} = Z_0$ and α, β are the bifurcation parameters discussed above.

From parameters $\alpha = \alpha(Z)$ and $\beta = \beta(Z)$ we can obtain all the bifurcations of the degenerate cycle Γ_0, of Z_0 in $\mathcal{V}_0$. Consider $Z_0 \in \mathcal{V}_0$ satisfying $BS(1)$-$BS(3)$ and $BSC(1)$-$BSC(2)$. From the previous sections there are six cases to analyze:

- DSC_{11}: Z_0 has a saddle-regular point of type BS_1 and the hyperbolicity ratio of X_0 is greater than one;
- DSC_{12}: Z_0 has a saddle-regular point of type BS_1 and the hyperbolicity ratio of X_0 is smaller than one;
- DSC_{21}: Z_0 has a saddle-regular point of type BS_2 and the hyperbolicity ratio of X_0 is greater than one;
- DSC_{22}: Z_0 has a saddle-regular point of type BS_2 and the hyperbolicity ratio of X_0 is smaller than one;
- DSC_{31}: Z_0 has a saddle-regular point of type BS_3 and the hyperbolicity ratio of X_0 is greater than one;

  - DSC_{32}: Z_0 has a saddle-regular point of type BS_3 and the hyperbolicity ratio of X_0 is smaller than one.

All the cases have at least four bifurcation curves in the (α, β)-plane, given implicitly as functions of α and β. To describe the codimension 1 phenomena curves we identify Σ with $\mathbb{R}$.

  - For $Z = (X, Y) \in \mathcal{V}_0$, let $P_E(Z)$ be the point $\Sigma \cap PE_Z$ and PE_Z is the curve where X is parallel to Y. Let γ_{P_E} be the curve implicitly defined by $\pi(a_{Z_{\alpha,\beta}}) - P_E(Z_{\alpha,\beta}) = 0$, i.e., $\gamma_{P_E} = \{(\alpha, \beta) \in \mathcal{B}_0; \pi(a_{Z_{\alpha,\beta}}) - P_E(Z_{\alpha,\beta}) = 0\}$. Then γ_{P_E} is the curve for which there exists a connection between the pseudo equilibrium and the point $(a_{Z_{\alpha,\beta}}, 0)$. Thus this curve lies either on the half plane $\beta > 0$ or in the half plane $\beta < 0$.
  - For $Z = (X, Y) \in \mathcal{V}_0$, let $F(Z)$ be the fold point of X in Σ near S_X. Remember that F_X is an invisible fold-regular point if $\beta(Z) > 0$, a visible fold-regular point if $\beta(Z) < 0$, and a saddle-regular point if $\beta(Z) = 0$. Define $\gamma_F = \{(\alpha, \beta) \in \mathcal{B}_0; \pi(a_{Z_{\alpha,\beta}}) - F(Z_{\alpha,\beta}) = 0\}$. Then γ_F is the curve providing a connection between the fold point $F_{X_{\alpha,\beta}}$ and the point $(a_{Z_{\alpha,\beta}}, 0)$. Since, for $\beta \leq 0$, $(a_{Z_{\alpha,\beta}}, 0)$ corresponds to the fold point of $Z_{\alpha,\beta}$, this curve coincides with the axis α.
  - For $Z = (X, Y) \in \mathcal{V}_0$, let $P_1(Z)$ be the points in Σ where the invariant manifolds of X at S_X cross Σ, as defined previously. Define the curve $\gamma_{P_1} = \{(\alpha, \beta) \in \mathcal{B}_0; \beta \geq 0 \text{ and } \pi(a_{Z_{\alpha,\beta}}) - P_1(Z_{\alpha,\beta}) = 0\}$ that provides a pseudo-homoclinic connection between $P_1(Z_{\alpha,\beta})$ and the saddle point.

These curves will be illustrated later in the bifurcation diagrams. In some cases extra bifurcation curves will emerge. To obtain an order relation between the curves, we denote, with some abuse of terminology, $\gamma_j(\alpha, \beta) = \{(\alpha, \beta) \in \mathcal{B}_0; \pi(a_{Z_{\alpha,\beta}}) - j(Z_{\alpha,\beta}) = 0\}$, for $j = P_E, F, P_1$.

It is worthwhile to observe that proofs of the main results go further beyond the simple combination of the following two codimension one bifurcations: bifurcation of boundary saddles and bifurcation of homoclinic loop. Now we are ready to describe the bifurcation diagrams for the family $Z_{\alpha,\beta}$. The following three theorems concern cycles of types DSC_{11} and DSC_{12}.

Theorem A. *Suppose that Z_0 is of type DSC_{11} and $\beta > 0$. Then for a family $Z_{\alpha,\beta} = (X_{\alpha,\beta}, Y_{\alpha,\beta}) \in \mathcal{V}_0$, bifurcation curves, γ_{P_E}, γ_{P_1}, and γ_{P_F}, emerge from the origin, there exists an attracting pseudo-node, and the following statements hold:*

  (a) *if $(\alpha, \beta) \in R_7^1$, where $R_7^1 = \{(\alpha, \beta); 0 < \beta < \gamma_{P_E}(\alpha, \beta)\}$, then there exists a sliding polycycle passing through $S_{X_{\alpha,\beta}}$ and $P_E(Z_{\alpha,\beta})$, which contains two segments of sliding orbits;*
  (b) *if $(\alpha, \beta) \in \gamma_{P_E}$, then there exists a sliding polycycle passing through $S_{X_{\alpha,\beta}}$ and $P_E(Z_{\alpha,\beta})$, which contains just one segment of sliding orbit;*
  (c) *if $(\alpha, \beta) \in R_6^1 = \{(\alpha, \beta); \gamma_{P_E}(\alpha, \beta) < \beta < \gamma_{P_1}(\alpha, \beta)\}$, then there exists a sliding pseudo-cycle passing through $S_{X_{\alpha,\beta}}$;*
  (d) *if $(\alpha, \beta) \in \gamma_{P_1}$, then there exists a pseudo-cycle passing through $S_{X_{\alpha,\beta}}$;*
  (e) *if $(\alpha, \beta) \in R_5^1 = \{(\alpha, \beta); \gamma_{P_1}(\alpha, \beta) < \beta < \gamma_F(\alpha, \beta)\}$, then there exists a sliding pseudo-cycle passing through $S_{X_{\alpha,\beta}}$;*
  (f) *if $(\alpha, \beta) \in \gamma_F$, then there exists a sliding pseudo-polycycle passing through $S_{X_{\alpha,\beta}}$ and $F(Z_{\alpha,\beta})$;*

(g) *if $(\alpha, \beta) \in R_4^1 = \{(\alpha, \beta); \gamma_F(\alpha, \beta) < \beta \text{ and } \alpha < 0\}$, then there exists a sliding pseudo-cycle passing through $S_{X_{\alpha,\beta}}$;*

(h) *if $\alpha = 0$ and $\beta > 0$, then there exists an attracting degenerate cycle passing through $S_{X_{\alpha,\beta}}$;*

(i) *if $(\alpha, \beta) \in R_3^1 = \{(\alpha, \beta); \beta > 0 \text{ and } \alpha > 0\}$, then there exists an attracting limit cycle through Σ^c.*

The bifurcation diagram is illustrated in Figure 11.

Proof. For $\beta > 0$ we have a real saddle $S_{X_{\alpha,\beta}}$. Since Z_0 is in the case DSC_{11}, the saddle-regular point of Z_0 is in the case BS_1, so there exists an attracting pseudo-node, $P_E(Z_{\alpha,\beta})$, satisfying $P_E(Z_{\alpha,\beta}) < P_1(Z_{\alpha,\beta})$ in Σ. Also, $P_1(Z_{\alpha,\beta}) < F(Z_{\alpha,\beta}) < P_2(Z_{\alpha,\beta})$ and, for $i = 1, 2, E$, $\lim\limits_{(\alpha,\beta) \to (0,0)} F(Z_{\alpha,\beta}) = \lim\limits_{(\alpha,\beta) \to (0,0)} P_i(Z_{\alpha,\beta}) = 0^-$. So, the curves γ_{F_Z}, γ_{P_1}, and γ_F emerge from the origin and lie on $\{(\alpha, \beta); \alpha < 0 \text{ and } \beta > 0\}$. The existence of the limit cycle follows from Proposition 3. The result follows by analyzing the dynamics of the system for the possible values of $\pi_{Z_{\alpha,\beta}}(a_{Z_{\alpha,\beta}})$. $\qquad\square$

Theorem B. *Suppose that Z_0 is of type DSC_{12} and $\beta > 0$. Then for a family $Z_{\alpha,\beta} = (X_{\alpha,\beta}, Y_{\alpha,\beta}) \in \mathcal{V}_0$, bifurcation curves, γ_{P_E}, γ_{P_1}, and γ_{P_F}, emerge from the origin, there exists an attracting pseudo-node, and the following statements hold:*

(a) *if $(\alpha, \beta) \in R_7^1$, where $R_7^1 = \{(\alpha, \beta); 0 < \beta < \gamma_{P_E}(\alpha, \beta)\}$, then a repelling limit cycle through Σ^c coexists with a sliding polycycle passing through $S_{X_{\alpha,\beta}}$ and $P_E(Z_{\alpha,\beta})$, which contains two segments of sliding orbits;*

(b) *if $(\alpha, \beta) \in \gamma_{P_E}$, then a repelling limit cycle through Σ^c coexists with a sliding polycycle passing through $S_{X_{\alpha,\beta}}$ and $P_E(Z_{\alpha,\beta})$, which contains only one segment of sliding orbit;*

(c) *if $(\alpha, \beta) \in R_6^1 = \{(\alpha, \beta); \gamma_{P_E}(\alpha, \beta) < \beta < \gamma_{P_1}(\alpha, \beta)\}$, then a repelling limit cycle through Σ^c coexists with a sliding pseudo-cycle passing through $S_{X_{\alpha,\beta}}$;*

(d) *if $(\alpha, \beta) \in \gamma_{P_1}$, then a repelling limit cycle through Σ^c coexists with a pseudo-cycle passing through $S_{X_{\alpha,\beta}}$;*

(e) *if $(\alpha, \beta) \in R_5^1 = \{(\alpha, \beta); \gamma_{P_1}(\alpha, \beta) < \beta < \gamma_F(\alpha, \beta)\}$, then a repelling limit cycle through Σ^c coexists with a sliding pseudo-cycle passing through $S_{X_{\alpha,\beta}}$;*

(f) *if $(\alpha, \beta) \in \gamma_F$, then a repelling limit cycle through Σ^c coexists with a sliding pseudo-polycycle passing through $S_{X_{\alpha,\beta}}$ and $F(Z_{\alpha,\beta})$;*

(g) *if $(\alpha, \beta) \in R_4^1 = \{(\alpha, \beta); \gamma_F(\alpha, \beta) < \beta \text{ and } \alpha < 0\}$, then a repelling limit cycle through Σ^c coexists with a sliding pseudo-cycle passing through $S_{X_{\alpha,\beta}}$;*

(h) *if $\alpha = 0$ and $\beta > 0$, then there exists a repelling degenerate cycle passing through $S_{X_{\alpha,\beta}}$;*

(i) *if $(\alpha, \beta) \in R_3^1 = \{(\alpha, \beta); \beta > 0 \text{ and } \alpha > 0\}$ then no cycle was detected.*

The bifurcation diagram is illustrated in Figure 12.

Proof. The proof is identical to the proof of Theorem A except that, as seen in Proposition 3, limit cycles appear for $\alpha < 0$ and the degenerate cycle for $\alpha = 0$ is a repeller. $\qquad\square$
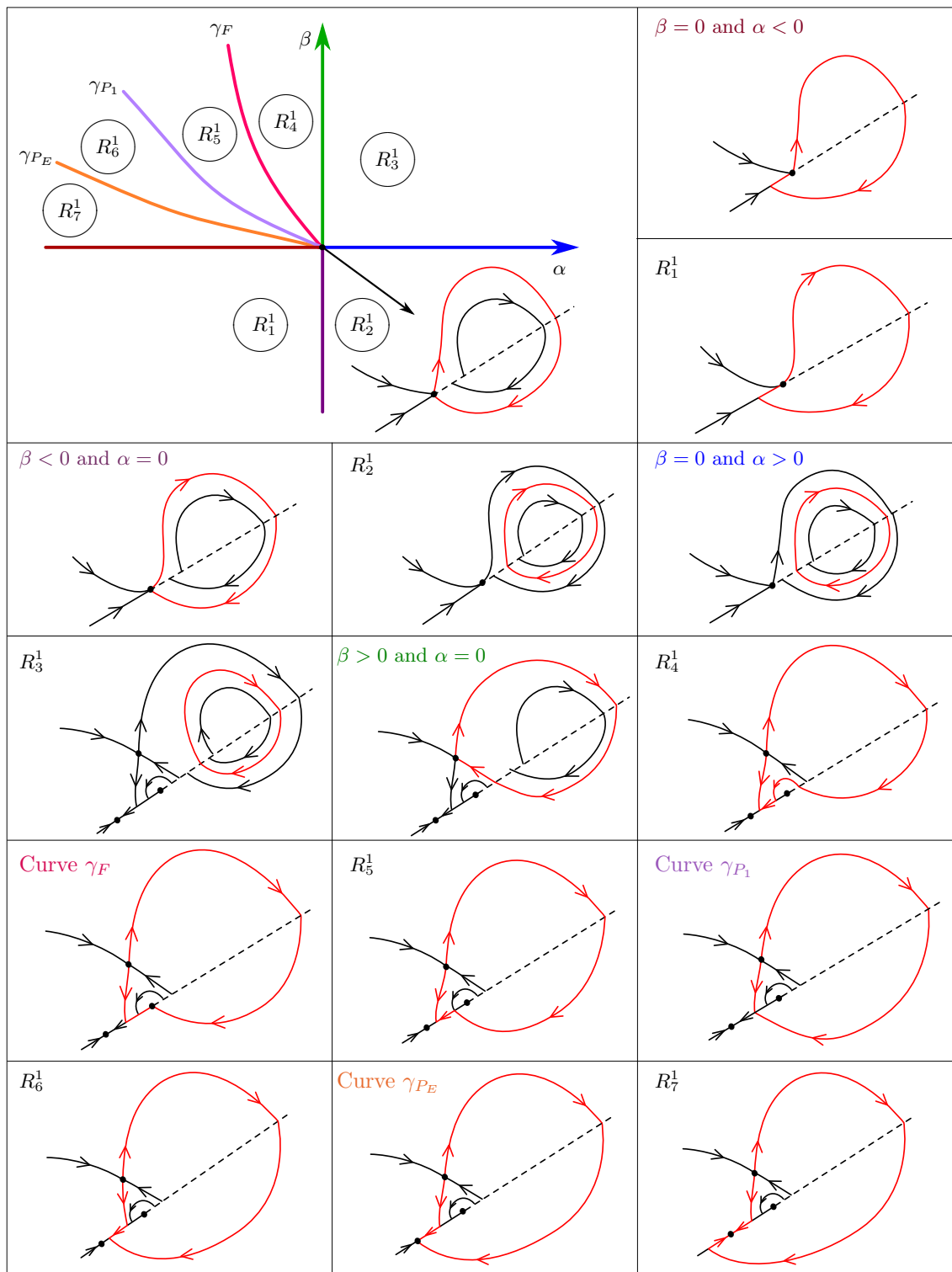
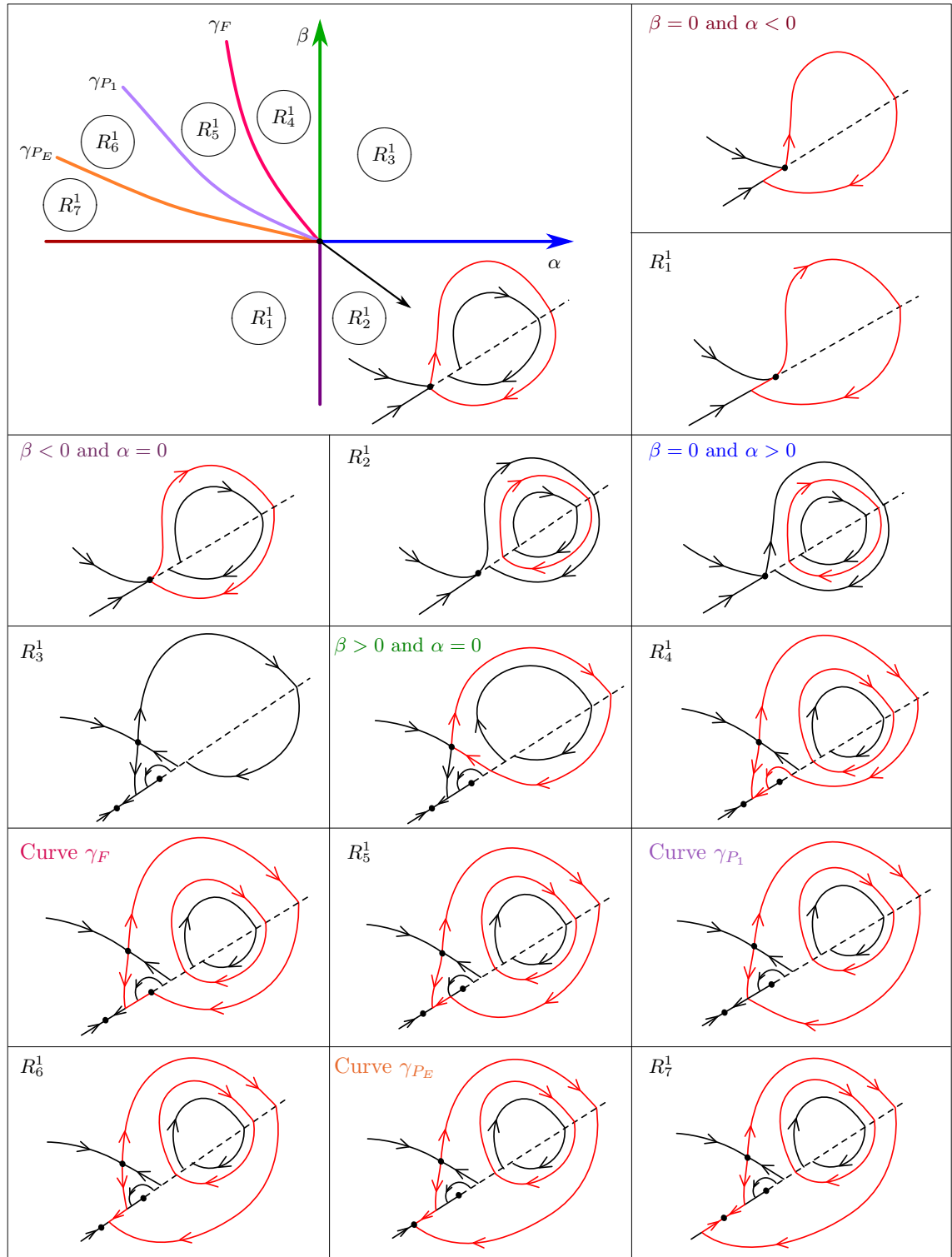FIGURE 11. Bifurcation diagram of $Z_{\alpha,\beta}$: case DSC_{11}.

18

FIGURE 12. Bifurcation diagram of $Z_{\alpha,\beta}$: case DSC_{12}.

Theorem C. *Suppose that Z_0 is of type DSC_{11} or DSC_{12} and $\beta \leq 0$. Then for a family $Z_{\alpha,\beta} = (X_{\alpha,\beta}, Y_{\alpha,\beta}) \in \mathcal{V}_0$ there exists no pseudo-equilibrium, $S_{X_{\alpha,\beta}}$ is as attractor for the sliding vector field, and:*

(a) *if $\beta = 0$ and $\alpha < 0$, then there exists a sliding cycle passing through the $S_{X_{\alpha,\beta}}$;*

(b) *if $\alpha = 0 = \beta$, then there exists an attractor polycycle passing through $S_{X_{0,0}}$;*

(c) *if $\beta = 0$ and $\alpha > 0$, then there exists an attracting limit cycle through Σ^c;*

(d) *if $(\alpha, \beta) \in R_1^1 = \{(\alpha,\beta); \beta < 0 \text{ and } \alpha < 0\}$, then there exists a sliding cycle passing through the fold-regular point $F(Z_{\alpha,\beta})$;*

(e) *if $\alpha = 0$ and $\beta < 0$, then there exists a degenerate cycle passing through the fold-regular point $F(Z_{\alpha,\beta})$;*

(f) *if $(\alpha, \beta) \in R_2^1 = \{(\alpha,\beta); \beta < 0 \text{ and } \alpha > 0\}$, then there exists an attracting limit cycle through Σ^c.*

The bifurcation diagrams for DSC_{11} and DSC_{12} are illustrated in Figures 11 and 12, respectively.

Proof. If $\beta = 0$ then $F(Z_{\alpha,\beta}) = S_{X_{\alpha,\beta}} \in \Sigma$. Items b and c follow directly from Proposition 3. If $\alpha < 0$ then the unstable manifold of the saddle in Σ^+ intersects Σ, after that it follows the flow of $Y_{\alpha,0}$ and it intersects the sliding region. Since $F(Z_{\alpha,\beta})$ is an attractor for the sliding vector field (see the bifurcation of a saddle-regular point of type BS_1), then there exists a sliding cycle through the saddle-regular point. If $\beta < 0$, then the saddle is virtual and there is no pseudo-equilibrium, the only distinguished singularity is the fold-regular point. The result follows similarly to the proof of Theorem B. $\qquad\square$

The following theorems concern cycles of type DSC_{21} and DSC_{22}.

Theorem D. *Suppose that Z_0 is of type DSC_{21}. Then for a family $Z_{\alpha,\beta} = (X_{\alpha,\beta}, Y_{\alpha,\beta}) \in \mathcal{V}_0$, bifurcation curves, γ_{P_E}, $\tilde{\gamma}_{P_E}$, γ_{P_1}, and γ_{P_F}, emerge from the origin and the following statements hold:*

1. *for $\beta \leq 0$: identical to the cases given in Theorem Cl*

2. *for $\beta > 0$: there exists an attracting pseudo-node and*

    (a) *if $(\alpha,\beta) \in R_8^2 = \{(\alpha,\beta); 0 < \beta < \gamma_{P_1}(\alpha,\beta)\}$, then there exists a sliding pseudo-cycle passing through $S_{X_{\alpha,\beta}}$;*

    (b) *if $(\alpha,\beta) \in \gamma_{P_1}$ then there exists a pseudo-cycle passing through $S_{X_{\alpha,\beta}}$;*

    (c) *if $(\alpha,\beta) \in R_7^2 = \{(\alpha,\beta); \gamma_{P_1}(\alpha,\beta) < \beta < \gamma_{P_E}(\alpha,\beta)\}$, then there exists a sliding pseudo-cycle passing through $S_{X_{\alpha,\beta}}$;*

    (d) *if $(\alpha,\beta) \in \gamma_{P_E}$, then there exists a sliding polycycle passing through $S_{X_{\alpha,\beta}}$ and $P_E(Z_{\alpha,\beta})$, which contains only one segment of sliding orbits;*

    (e) *if $(\alpha,\beta) \in R_6^2 = \{(\alpha,\beta); \gamma_{P_E}(\alpha,\beta) < \beta < \gamma_F(\alpha,\beta)\}$, then there exists a sliding polycycle passing through $S_{X_{\alpha,\beta}}$ and $P_E(Z_{\alpha,\beta})$, which contains two segments of sliding orbits;*

    (f) *if $(\alpha,\beta) \in \gamma_F$, then there exists a sliding polycycle passing through $S_{X_{\alpha,\beta}}$, $P_E(Z_{\alpha,\beta})$ and $F(Z_{\alpha,\beta})$;*

    (g) *if $(\alpha,\beta) \in R_5^2 = \{(\alpha,\beta); \gamma_F(\alpha,\beta) < \beta < \tilde{\gamma}_{P_E}(\alpha,\beta)\}$, then there exists a sliding pseudo-cycle passing through $S_{X_{\alpha,\beta}}$;*

    (h) *if $(\alpha,\beta) \in \tilde{\gamma}_{P_E}$ then there exists a sliding polycycle passing through $S_{X_{\alpha,\beta}}$ and $Q_{Z_{\alpha,\beta}}$, which contains only one sliding segment;*

(i) if $(\alpha, \beta) \in R_4^2 = \{(\alpha, \beta); \beta > \tilde{\gamma}_{P_E}(\alpha, \beta) \text{ and } \alpha < 0\}$, then there exists a sliding polycycle passing through $S_{X_{\alpha,\beta}}$ and $P_E(Z_{\alpha,\beta})$, which contains two sliding segments;

(j) if $\alpha = 0$ and $\beta > 0$, then there exists an attracting degenerate cycle through $S_{X_{\alpha,\beta}}$;

(k) if $(\alpha, \beta) \in R_3^2 = \{(\alpha, \beta); \beta > 0 \text{ and } \alpha > 0\}$, then there exists an attracting limit cycle passing through the crossing region near $P_{X_{\alpha,\beta}}$.

The bifurcation diagram is illustrated in Figure 13.

Proof. In the case DSC_{21}, the saddle-regular point satisfies case BS_2. The position of the curves γ_{P_E} and γ_{P_1} change between cases DSC_{11} and DSC_{12}, so that a new bifurcation curve, $\tilde{\gamma}_{P_E}$, emerges from the origin in the half plane where $\beta > 0$. Since $\alpha < 0$ and $\gamma_F < \beta < 0$, then $F(Z_{\alpha,\beta}) < \pi_{Z_{\alpha,\beta}}(a_{Z_{\alpha,\beta}}) < a_{Z_{\alpha,\beta}}$, the trajectory that contains the unstable manifold of the saddle crosses the crossing region twice before reaching the sliding region from Σ^+. Therefore, by continuity, there exist values of α and β so that this trajectory reaches Σ^s at the pseudo-equilibrium point. This new curve provides a connection between $S_{X_{\alpha,\beta}}$ and $P_E(Z_{\alpha,\beta})$. The rest of the proof is similar to the proof of Theorem A. $\qquad\square$

Theorem E. *Suppose that Z_0 is of type DSC_{22}. Then for a family $Z_{\alpha,\beta} = (X_{\alpha,\beta}, Y_{\alpha,\beta}) \in \mathcal{V}_0$, bifurcation curves, γ_{P_E}, $\tilde{\gamma}_{P_E}$, γ_{P_1}, and γ_{P_F}, emerge from the origin and the following statements hold:*

1. *for $\beta \leq 0$: identical to the cases given in Theorem C.*
2. *for $\beta > 0$: there exists a pseudo-node which is an attractor for the sliding vector field and:*

    (a) *if $(\alpha, \beta) \in R_8^2 = \{(\alpha, \beta); 0 < \beta < \gamma_{P_1}(\alpha, \beta)\}$, then a repelling limit cycle through Σ^c coexists with a sliding pseudo-cycle passing through $S_{X_{\alpha,\beta}}$;*

    (b) *if $(\alpha, \beta) \in \gamma_{P_1}$ then a repelling limit cycle through Σ^c coexists with a pseudo-cycle passing through $S_{X_{\alpha,\beta}}$;*

    (c) *if $(\alpha, \beta) \in R_7^2 = \{(\alpha, \beta); \gamma_{P_1}(\alpha, \beta) < \beta < \gamma_{P_E}(\alpha, \beta)\}$, then a repelling limit cycle through Σ^c coexists with a sliding pseudo-cycle passing through $S_{X_{\alpha,\beta}}$;*

    (d) *if $(\alpha, \beta) \in \gamma_{P_E}$, then a repelling limit cycle through Σ^c coexists with a sliding polycycle passing through $S_{X_{\alpha,\beta}}$ and $P_E(Z_{\alpha,\beta})$, which contains only one segment of sliding orbits;*

    (e) *if $(\alpha, \beta) \in R_6^2 = \{(\alpha, \beta); \gamma_{P_E}(\alpha, \beta) < \beta < \gamma_F(\alpha, \beta)\}$, then a repelling limit cycle through Σ^c coexists with a sliding polycycle passing through $S_{X_{\alpha,\beta}}$ and $P_E(Z_{\alpha,\beta})$, which contains two segments of sliding orbits;*

    (f) *if $(\alpha, \beta) \in \gamma_F$, then a repelling limit cycle through Σ^c coexists with a sliding polycycle passing through $S_{X_{\alpha,\beta}}$, $P_E(Z_{\alpha,\beta})$ and $F(Z_{\alpha,\beta})$;*

    (g) *if $(\alpha, \beta) \in R_5^2 = \{(\alpha, \beta); \gamma_F(\alpha, \beta) < \beta < \tilde{\gamma}_{P_E}(\alpha, \beta)\}$, then a repelling limit cycle through Σ^c coexists with a sliding pseudo-cycle passing through $S_{X_{\alpha,\beta}}$;*

    (h) *if $(\alpha, \beta) \in \tilde{\gamma}_{P_E}$, a repelling limit cycle through Σ^c coexists with a sliding polycycle passing through $S_{X_{\alpha,\beta}}$ and $Q_{Z_{\alpha,\beta}}$, which contains only one sliding segment;*

(i) if $(\alpha, \beta) \in R_4^2 = \{(\alpha, \beta); \beta > \tilde{\gamma}_{P_E}(\alpha, \beta) \text{ and } \alpha < 0\}$, then a repelling limit cycle through Σ^c coexists with a sliding polycycle passing through $S_{X_{\alpha,\beta}}$ and $P_E(Z_{\alpha,\beta})$, which contains two sliding segments;

(j) if $\alpha = 0$ and $\beta > 0$, then there exists a repelling degenerate cycle through $S_{X_{\alpha,\beta}}$;

(k) if $(\alpha, \beta) \in R_3^2 = \{(\alpha, \beta); \beta > 0 \text{ and } \alpha > 0\}$, then no cycle was detected.

The bifurcation diagram is illustrated in Figure 14.

Proof. The only difference from the proof of Theorem A is the position of the limit cycles given in Proposition 3. $\qquad \square$

The following theorems concern the last two cases, DSC_{31} and DSC_{32}.

Theorem F. *Suppose that Z_0 is in the case DSC_{31} and $\beta > 0$. Then for a family $Z_{\alpha,\beta} = (X_{\alpha,\beta}, Y_{\alpha,\beta}) \in \mathcal{V}_0$, bifurcation curves, γ_{P_1} and γ_{P_F} emerge from the origin, there exists no pseudo-equilibrium, $S_{X_{\alpha,\beta}}$ is a repeller for the sliding vector field, and the following statements hold:*

(a) *if $(\alpha, \beta) \in R_7^1$, where $R_7^3 = \{(\alpha, \beta); 0 < \beta < \gamma_{P_1}(\alpha, \beta)\}$, then there exists a sliding pseudo-cycle through $S_{X_{\alpha,\beta}}$;*

(b) *if $(\alpha, \beta) \in \gamma_{P_1}$, then there exists a pseudo-cycle passing through $S_{X_{\alpha,\beta}}$;*

(c) *if $(\alpha, \beta) \in R_6^3 = \{(\alpha, \beta); \gamma_{P_1}(\alpha, \beta) < \beta < \gamma_F(\alpha, \beta)\}$, then there exists a sliding pseudo-cycle through $S_{X_{\alpha,\beta}}$;*

(d) *if $(\alpha, \beta) \in \gamma_F$, then there exists a sliding pseudo-polycycle through $S_{X_{\alpha,\beta}}$ and $F(Z_{\alpha,\beta})$;*

(e) *if $(\alpha, \beta) \in R_5^3 = \{(\alpha, \beta); \gamma_F(\alpha, \beta) < \beta \text{ and } \alpha < 0\}$, then there exists a sliding pseudo-cycle through $S_{X_{\alpha,\beta}}$;*

(f) *if $\alpha = 0$ and $\beta > 0$, then there exists an attracting degenerate cycle through $S_{X_{\alpha,\beta}}$;*

(g) *if $(\alpha, \beta) \in R_4^3 = \{(\alpha, \beta); \beta > 0 \text{ and } \alpha > 0\}$, then there exists a limit cycle passing through Σ^s.*

The bifurcation diagram is illustrated in Figure 15.

Proof. Since Z_0 is in case DSC_{31}, the saddle-regular point is of type BS_3, i.e., the pseudo-equilibrium points appear when the saddle is virtual ($\beta < 0$). Thus, there is no pseudo-equilibrium for $\beta > 0$. The position of the limit cycles given in Proposition 3 implies that they happen for $\alpha > 0$. The rest of the proof is similar to the proof of Theorem A. $\qquad \square$
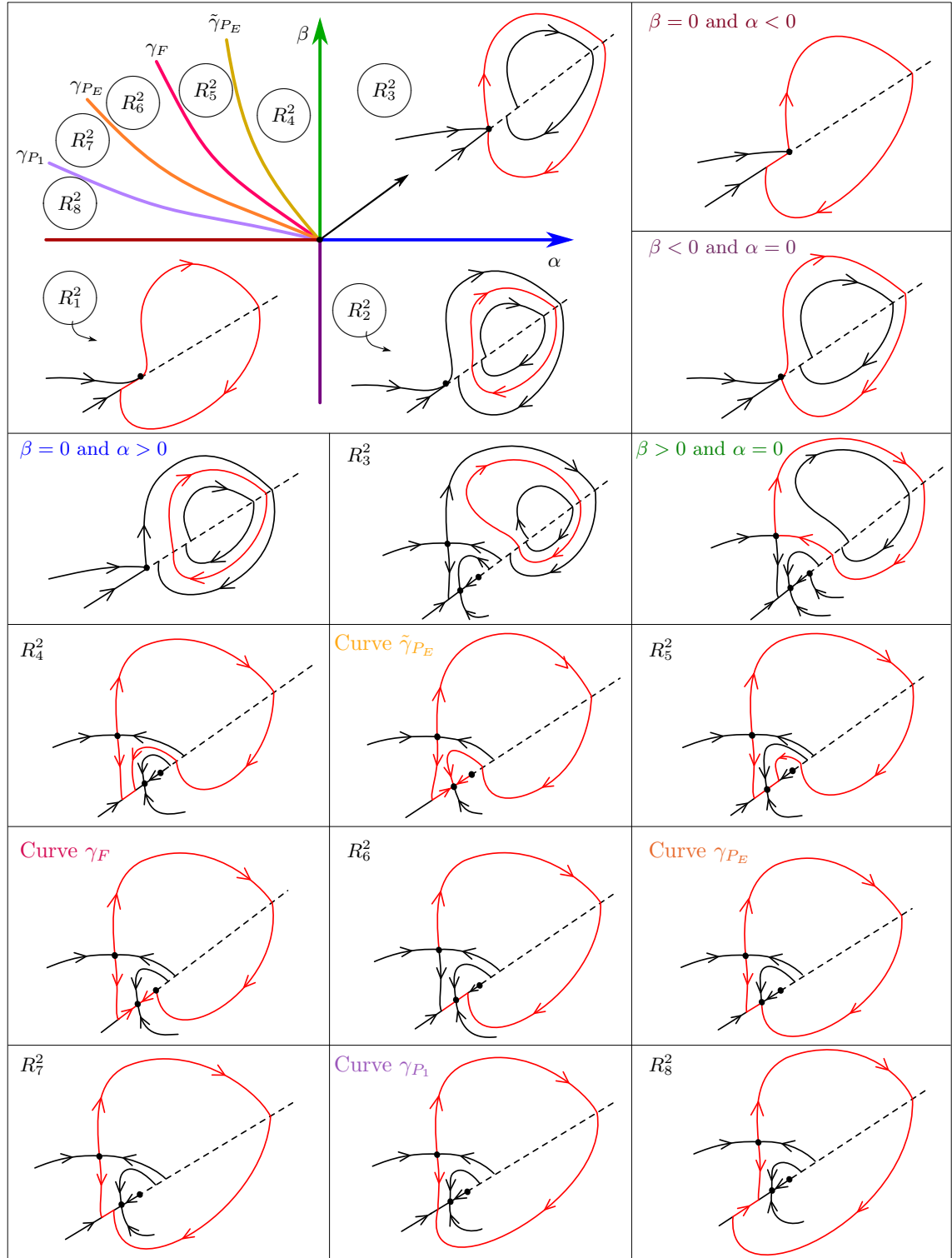
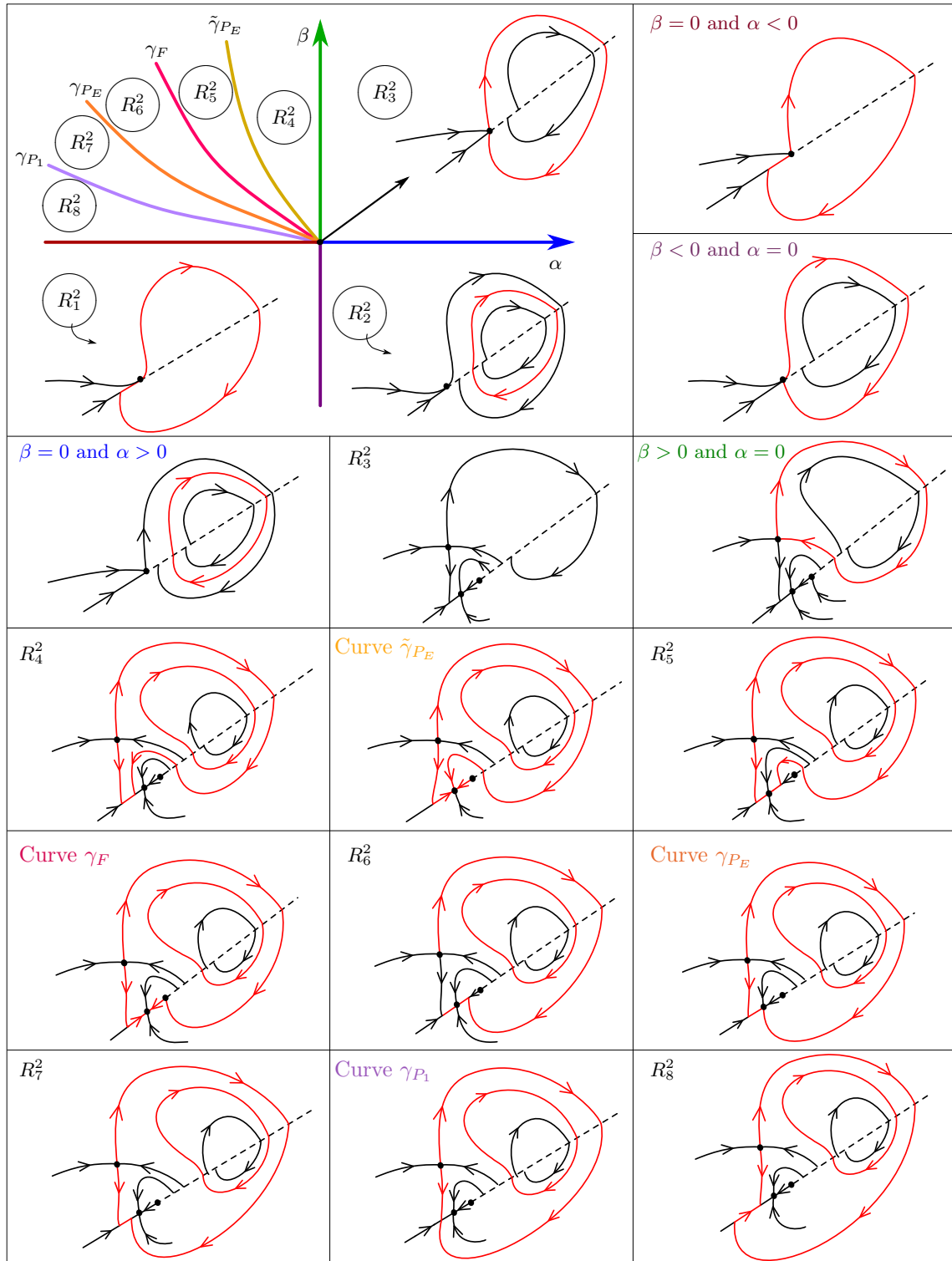FIGURE 13. Bifurcation diagram of $Z_{\alpha,\beta}$: case DSC_{21}.

FIGURE 14. Bifurcation diagram of $Z_{\alpha,\beta}$: case DSC_{22}.

Theorem G. *Suppose that Z_0 is in the case DSC_{32} and $\beta > 0$. Then for a family $Z_{\alpha,\beta} = (X_{\alpha,\beta}, Y_{\alpha,\beta}) \in \mathcal{V}_0$, bifurcation curves, γ_{P_1} and γ_{P_F} emerge from the origin, there exists no pseudo-equilibrium, $S_{X_{\alpha,\beta}}$ is a repeller for the sliding vector field, and the following statements hold:*

(a) *if $(\alpha, \beta) \in R_7^1$, where $R_7^3 = \{(\alpha, \beta); 0 < \beta < \gamma_{P_1}(\alpha, \beta)\}$, then a repelling limit cycle through Σ^c coexists with a sliding pseudo-cycle through $S_{X_{\alpha,\beta}}$;*

(b) *if $(\alpha, \beta) \in \gamma_{P_1}$, then a repelling limit cycle through Σ^c coexists with a pseudo-cycle passing through $S_{X_{\alpha,\beta}}$;*

(c) *if $(\alpha, \beta) \in R_6^3 = \{(\alpha, \beta); \gamma_{P_1}(\alpha, \beta) < \beta < \gamma_F(\alpha, \beta)\}$, then a repelling limit cycle through Σ^c coexists with a sliding pseudo-cycle through $S_{X_{\alpha,\beta}}$;*

(d) *if $(\alpha, \beta) \in \gamma_F$, then a repelling limit cycle through Σ^c coexists with a sliding pseudo-polycycle through $S_{X_{\alpha,\beta}}$ and $F(Z_{\alpha,\beta})$;*

(e) *if $(\alpha, \beta) \in R_5^3 = \{(\alpha, \beta); \gamma_F(\alpha, \beta) < \beta$ and $\alpha < 0\}$, then a repelling limit cycle through Σ^c coexists with a sliding pseudo-cycle through $S_{X_{\alpha,\beta}}$;*

(f) *if $\alpha = 0$ and $\beta > 0$, then there exists a repelling degenerate cycle through $S_{X_{\alpha,\beta}}$;*

(g) *if $(\alpha, \beta) \in R_4^3 = \{(\alpha, \beta); \beta > 0$ and $\alpha > 0\}$, then no cycle was detected.*

The bifurcation diagram is illustrated in Figure 16.

Proof. The position of the limit cycles given in Proposition 3 implies that they happen for $\alpha < 0$. The rest of the proof is similar to the proof of Theorem F. □

**Theorem H.** *Suppose that Z_0 is in the case DSC_{31} or DSC_{32} and $\beta \le 0$. Then the a $Z_{\alpha,\beta} = (X_{\alpha,\beta}, Y_{\alpha,\beta}) \in \mathcal{V}_0$ satisfies: there exists no pseudo-equilibrium, $S_{X_{\alpha,\beta}}$ is an attractor for the sliding vector field, and:*

(a) *if $\beta = 0$ and $\alpha < 0$, then there exists a sliding cycle passing through the $S_{X_{\alpha,\beta}}$;*

(b) *if $\alpha = 0 = \beta$, then there exists an attracting degenerate cycle passing through $S_{X_{0,0}}$;*

(c) *if $\beta = 0$ and $\alpha > 0$, then there exists an attracting limit cycle through Σ^c;*

(d) *if $(\alpha, \beta) \in R_1^3 = \{(\alpha, \beta); \gamma_{P_E}(\alpha, \beta) < \beta < 0\}$, then there exists a sliding cycle passing through the fold-regular point $F(Z_{\alpha,\beta})$;*

(e) *if $(\alpha, \beta) \in \gamma_{P_E}$, there exists a polycycle passing through $F(Z_{\alpha,\beta})$ and $P_E(Z_{\alpha,\beta})$;*

(f) *if $(\alpha, \beta) \in R_2^3 = \{(\alpha, \beta); \alpha < 0$ and $\beta < \gamma_{P_E}(\alpha, \beta)\}$, then there exists a sliding cycle passing through $P_{X_{\alpha,\beta}}$;*

(g) *if $\alpha = 0$ and $\beta < 0$, then an attracting degenerate cycle through $F(Z_{\alpha,\beta})$;*

(h) *if $(\alpha, \beta) \in R_3^3 = \{(\alpha, \beta); \beta < 0$ and $\alpha > 0\}$, then there exists an attracting limit cycle through Σ^+.*

The bifurcation diagram for DSC_{31} and DSC_{32} are illustrated in Figures 15 and 16, respectively.

Proof. The position of the limit cycles given in Proposition 3 implies that they happen for $\alpha > 0$. The rest of the proof is similar to the proof of Theorem A. □
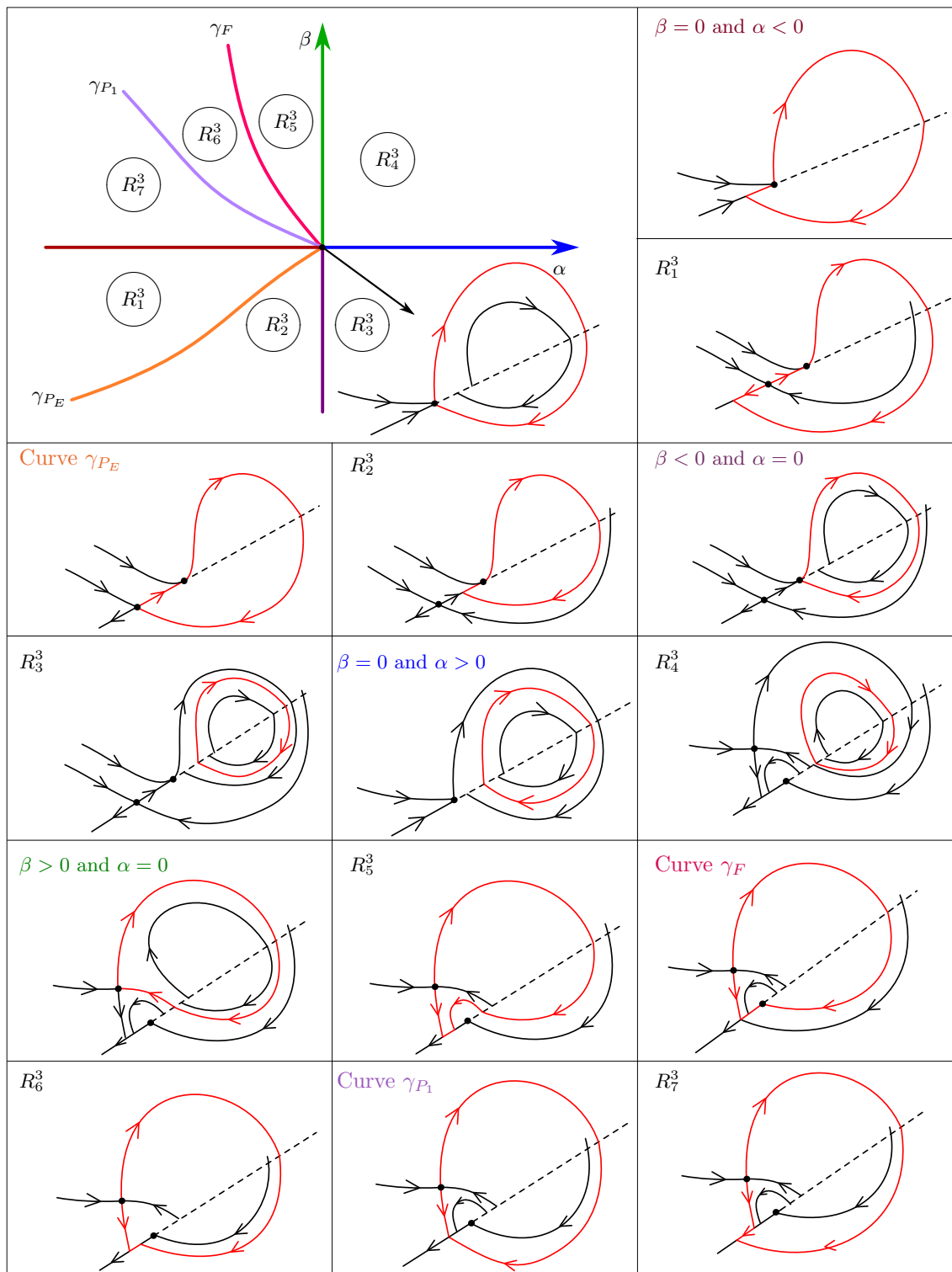
FIGURE 15. Bifurcation diagram of $Z_{\alpha,\beta}$: case DSC_{31}.
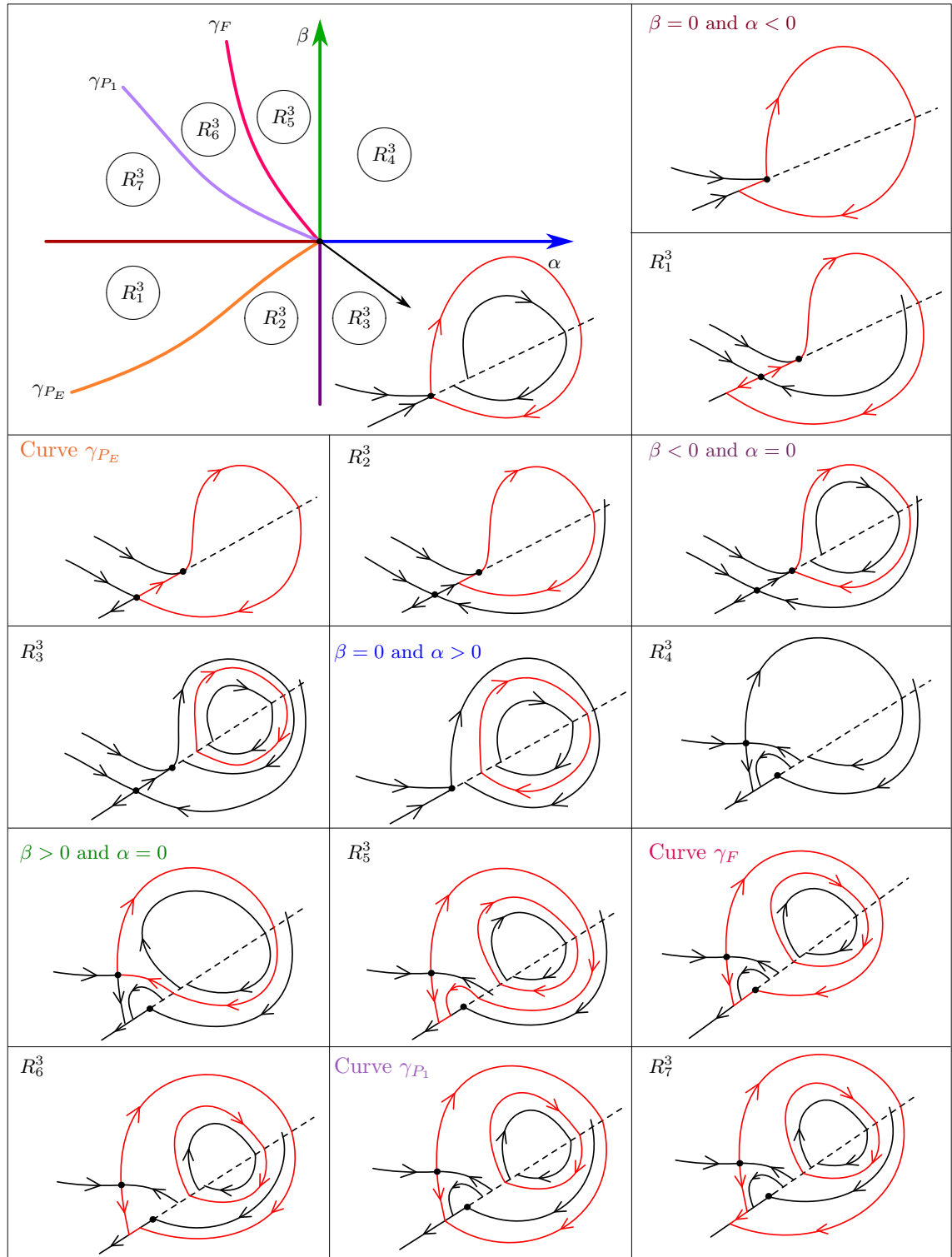
FIGURE 16. Bifurcation diagram of $Z_{\alpha,\beta}$: case DSC_{32}.

5. The Resonant Case

5.1. **Class of Vector Fields with Hyperbolicity Ratio $= 1$.** Let $\mathcal{A}$ be the set of all nonsmooth vector fields $Z = (X, Y) \in \Omega^l$, $l > 1$ big enough for our proposes, where X has a hyperbolic saddle S_X and, in a neighborhood of S_X, X is $\mathcal{C}^2$-conjugated to a vector field $W(\mathbf{x}) = A\mathbf{x} + \mathbf{c}$, where

$$(4) \qquad A = \begin{pmatrix} 0 & a \\ b & 0 \end{pmatrix} \quad \text{and} \quad \mathbf{c} = \begin{pmatrix} -a\tilde{y} \\ -b\tilde{x} \end{pmatrix}$$

with $a, b > 0$, $S_X = (\tilde{x}, \tilde{y})$, and $\Sigma = h^{-1}(0)$ where $h(x, y) = y$. This conjugacy preserves the discontinuity set Σ. The eigenvalues of A in equation 4 are $\pm\sqrt{ab}$, therefore, for all $Z \in \mathcal{A}$, the hyperbolicity ratio of any S_X is equal to 1.

By considering vector fields in $\mathcal{V}_{Z_0} \cap \mathcal{A}$ we now perform an analysis of the first return map. We proceed similarly to the analysis performed for the case $r \notin \mathbb{Q}$. The main difference is that we consider Σ fixed and the saddle point variable. Then for each $Z \in \mathcal{V}_{Z_0} \cap \mathcal{A}$, there is no loss of generality in assuming $a_Z = 0$ (this is possible up to translation maps) and the image of a_Z by conjugacy is also 0 (this is possible because the conjugacy preserves Σ).

Let $\tau \subset \Sigma^+$ be a transversal section to the flow of X such that, if $S_X \in \Sigma^+$, then τ is above S_X. In this case, the transition map of X near S_X is $\rho_1 : [0, \delta_Z) \to \sigma$ with $\rho_1(x)$ being the projection on the first coordinate of the point where the trajectory of X passing through $(x, 0) \in [0, \delta_Z) \times \{0\}$ meets τ at the first (positive) time. Let $\tau_W \subset \{(x, \varepsilon) \in \mathbb{R}^2\}$ be the transversal section to the flow of W for some $\varepsilon > 0$, such that this section is contained in the neighborhood where W and X are conjugated. Without loss of generality we assume that τ is the image by conjugacy of σ_W.

Lemma 2. *The transition map $\rho_W : [0, \delta) \to \sigma_W$ can be differentially extended to an open neighborhood of 0.*

Proof. The trajectories of W lie in the level curves of the function $G(x, y) = bx^2 - ay^2 + 2c_1 x - 2c_2 y$, where $c_1 = -b\tilde{x}$ and $c_2 = -a\tilde{y}$. Assume that ρ_W is defined for $0 \le x < \delta$. For each $(x, 0) \in \Sigma$ with $0 \le x < \delta$ we obtain

$$(5) \qquad \rho_W(x) = -\frac{c_1}{b} + \sqrt{x^2 + \frac{2c_1}{b}x + \frac{a}{b}\varepsilon^2 + \frac{2c_2}{b}\varepsilon + \frac{c_1^2}{b^2}}.$$

The x-independent part of the expression inside the square root, $Q(\varepsilon) = \dfrac{a}{b}\varepsilon^2 + \dfrac{2c_2}{b}\varepsilon + \dfrac{c_1^2}{b^2}$, is a polynomial of degree 2 in ε. We analyze this polynomial in three different cases:

- (i) If $\tilde{y} < 0$ we have $c_2 > 0$. As $P_X = (0, 0)$ we must have $c_1 = 0$ and since $a, b > 0$ it follows that $Q(\varepsilon) > 0$ for $\varepsilon > 0$.
- (ii) If $\tilde{y} = 0$ then $S_X = (0, 0)$, consequently $c_1 = c_2 = 0$ and $Q(\varepsilon) > 0$ for $\varepsilon > 0$.
- (iii) If $\tilde{y} > 0$, then $c_2 < 0$. Imposing the condition that the stable manifold of S_X intersects Σ in $(0, 0)$ we obtain $c_1 = -c_2\sqrt{b/a} > 0$. It implies that Q has only one root, which is $-c_2/a = \tilde{y}$ and $Q(\varepsilon) > 0$ for all $\varepsilon > 0$ and $\varepsilon \neq \tilde{y}$. However, for our proposes, $\varepsilon > \tilde{y}$. Thus, $Q(\varepsilon) > 0$ for $\varepsilon > \tilde{y}$.

Therefore, choosing $\varepsilon > \max\{0, \tilde{y}\}$ we obtain $Q(\varepsilon) > 0$, and we can find $\delta_W > 0$ such that the expression inside the square root in (5) is positive for $x \in (-\delta_W, \delta_W)$. It follows that ρ_W can be differentially extended to an open neighborhood of 0. $\square$

Since W is $\mathcal{C}^2$-conjugated to X in a neighborhood of S_X there exists a diffeomorphism of class $\mathcal{C}^2$-, ψ, defined in a neighborhood of S_X, such that $\psi(S_W) = S_X$ and

$$(6) \qquad \rho_1(x) = \psi \circ \rho_W \circ \psi^{-1}(x).$$

It follows from this expression that ρ_1 can be at least $\mathcal{C}^2$-extended to an open neighborhood of 0, allowing us to calculate the Taylor series of π_Z at $x = 0$ to order 2.

Proposition 4. *Consider $Z = (X, Y) \in \mathcal{A} \cap \mathcal{V}_{Z_0}$ and let $S_X = (\tilde{x}, \tilde{y})$ be the saddle point associated with X. Suppose that the first return map is defined in a half-open interval $[0, \delta_Z)$, for some $\delta_Z > 0$. Then the first return map of Z can be written as*

$$(7) \qquad \pi_Z(x) = \alpha + k_1(\beta)x + k_2(\beta)x^2 + \ h.o.t.,$$

where $0 < |k_1(\beta)| < 1$ if $\beta > 0$ and $k_1(\beta) = 0$, $k_2(\beta) > 0$ if $\beta \leq 0$.

Proof. The proof follows directly from Lemma 2 by calculating the derivatives of $\pi_Z(x) = \rho_3 \circ \rho_2 \circ \rho_1(x)$. $\qquad \square$

It follows from this result that for $\bar{Z}$ we have $\pi_{\bar{Z}}(0) = 0$, $\frac{d\pi_{\bar{Z}}}{dx}(0) = 0$ and $\frac{d^2\pi_{\bar{Z}}}{dx^2}(0) > 0$. Let Γ be the degenerate cycle of $\bar{Z}$. Since the first return map is only defined in a half-open interval, there exists a neighborhood of Γ such that the orbits of $\bar{Z}$ in this neighborhood, through points where the first return map is defined, having Γ as ω-limit set. Another consequence of this proposition, which has a similar proof as to that of Proposition 3, is the following.

Corollary 1. *Under the hypotheses in the Proposition 4, if $Z \in \mathcal{V}_{Z_0} \cap \mathcal{A}$ is such that $\alpha > 0$ then, for some $x > 0$ sufficiently small, Z has a stable limit cycle passing through $(x, 0) \in \Sigma$. If Z is such that $\alpha = 0$, then there exists a degenerate cycle Γ having a neighborhood for which the orbits of Z in this neighborhood passing through points where the first return map is defined have Γ as ω-limit set.*

Therefore, for $Z \in \mathcal{V}_{Z_0} \cap \mathcal{A}$ the first return π_Z has the graph equal to the graph for nonresonant saddles with hyperbolicity ratio smaller than 1. Therefore, depending on the structure of the local saddle-regular point, the bifurcation diagram in this case is given in Figure 11, or 13, or 15.

5.2. **Model with Hyperbolicity Ratio in** $\mathbb{Q}$. Now we consider a model with hyperbolicity ratio $r > 0$, and study how the system evolves for some values of $r \in \mathbb{Q}$. Consider $Z_a = (X_a, Y_a)$ with $a = (r, k, d, m)$, $\Sigma = h^{-1}(0)$, $h(x, y) = y + x/4 - m$, and

$$(8) \qquad X_a = \begin{pmatrix} x \\ -ry - x^3 - kx \end{pmatrix} \quad \text{and} \quad Y_a = \begin{pmatrix} -1 \\ -x + d \end{pmatrix}.$$

Observe that:

- For $r > 0$, $S_{X_a} = S = (0,0)$ is a hyperbolic saddle of X_a with hyperbolicity ratio r.
- $W^s(S, X_a) = \{(x, y) \in \mathbb{R}^2; x = 0\}$ and $W^s(S, X) = \left\{(x, y) \in \mathbb{R}^2; y = -\frac{x^3}{r+3} - \frac{kx}{r+1}\right\}$.

- $W^s(S, X_a) \cap \Sigma = P_2$ and $W^u(S, X_a) \cap \Sigma = \{P_4, P_1, P_3\}$, where $P_j = P_j(r, k, m) = (x_j, -x_j/4 + m)$, $j = 1, 3, 4$, $P_2 = (0, m)$ and $x_4 < x_1 < x_3$. If $m > 0$ then $x_1 > 0$, $x_1 < 0$ for $m < 0$, and $x_1 = 0$ if $m = 0$. Also, for $m = 0$, $x_4 = -\sqrt{\frac{(r+1-4k)(r+3)}{4(r+1)}}$ and $x_3 = \sqrt{\frac{(r+1-4k)(r+3)}{4(r+1)}}$. Then for $k < 0$, $W^u(S, X_a)$ crosses Σ in three different points if $m \approx 0$.
- $F_{Z_a} = (x_F, -x_F/4 + m)$ is the fold point of X_a near S for $m \neq 0$. F_{Z_a} is visible if $m > 0$ and invisible if $m < 0$.
- $F_d = \left(d - \frac{1}{4}, -\frac{d}{4} + \frac{1}{16} - m\right)$ is the unique fold point of Y_a, which is invisible.
- Given $p_0 = (x_0, -x_0/4 + m) \in \Sigma$, the trajectory of Y_a through p_0 meets Σ again at the point $(2d - 1/2 - x_0, (x_0 - 2d)/4 + 1/8 + m)$. In this case, consider $\rho_3(x_0) = 2d - 1/2 - x_0$.
- For $k < 0$, $m = 0$, and $d > 0$ S is a saddle-regular point of type BS_3.
- By considering Σ parametrized by the first coordinate $(x \mapsto (x, -x/4 + m))$, the sliding vector field is
$$Z^s(x) = -\frac{4x^3 + 4x^2 + (4k - 4d - r) + 4mr}{4x^3 - (5 - 4k + r)x + 4mr + 4d - 1}.$$

For any two points p_1 and p_2 in Σ, we can choose the parameter d so that they lie on the same trajectory of Y_a. Phase portraits of X_a and Y_a for $m = 0$, $r > 0$, and $k < 0$ are given in Figure 17.
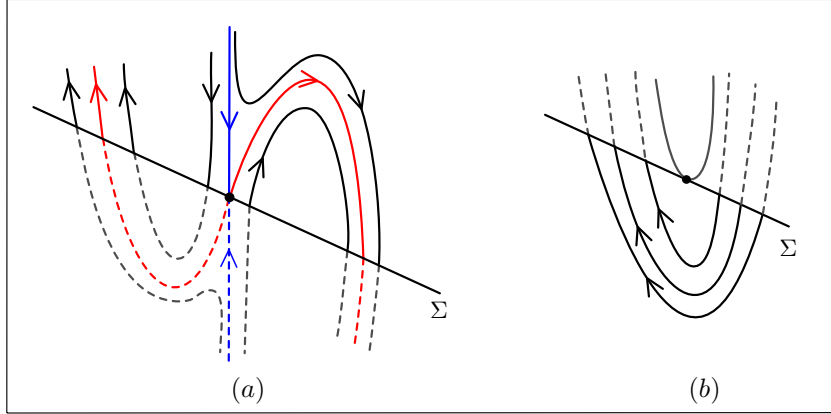
FIGURE 17. Phase portraits of (a) X_a and (b) Y_a with $m = 0$, $r > 0$, and $k < 0$.

In what follows, assume $r > 0$, $k < 0$, and $m \approx 0$ sufficiently small such that $W^u(S, X_a) \cap \Sigma = 3$. Fix $r > 0$ and $k, 0$, for each m, by varying d, we obtain all configurations given by the curves γ_F, γ_{P_1}, γ_{P_2}, and γ_{P_E}, depending on the signal of m. By changing m and d we want to show that Z_a realizes the bifurcation diagram DSC_{31} if $r > 1$ or DSC_{32} if $r < 1$. To do so it is enough to show the existence of the limit cycles given in that bifurcation diagrams, and that the pseudo-equilibria appear when $m > 0$, i.e., when the saddle is virtual. Since a full account of the algebraic cases is not feasible, we illustrate them numerically.

Graphs of the first return map for some values of the parameters were obtained numerically. All graphs are given with the variable x having an initial point at the corresponding a_Z for which the first return is defined. See Figures 18, 20, and 22 for some values of $r \in \mathbb{Q}$ satisfying $0 < r < 1$ and see Figures 19, 21,

and 23 for some values of $r \in \mathbb{Q}$ with $r > 1$. For each m fixed, the first return map varies continuously as the other parameters vary, implying that the results for nonresonant saddles remains true for this model. By performing a numerical analysis of the pseudo-equilibrium, we have that the bifurcations of the degenerate cycles obey bifurcation diagrams given in Figure 15 if $r > 1$ and Figure 16 if $r < 1$.
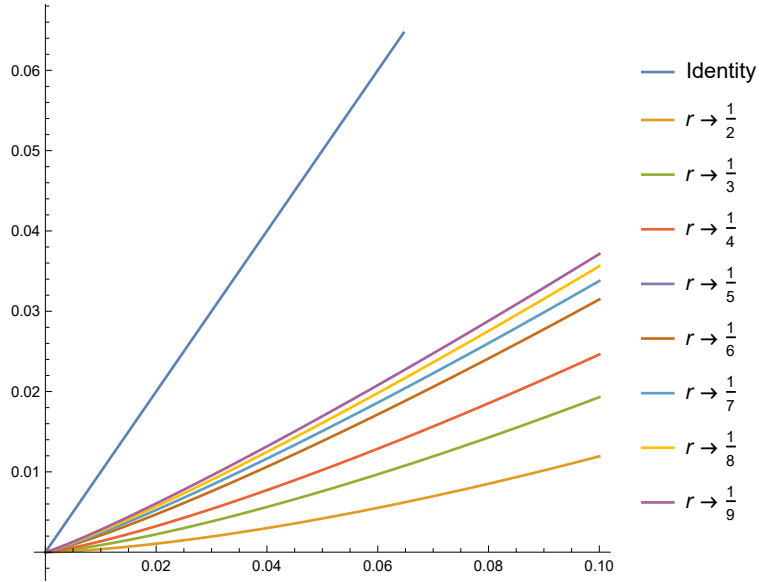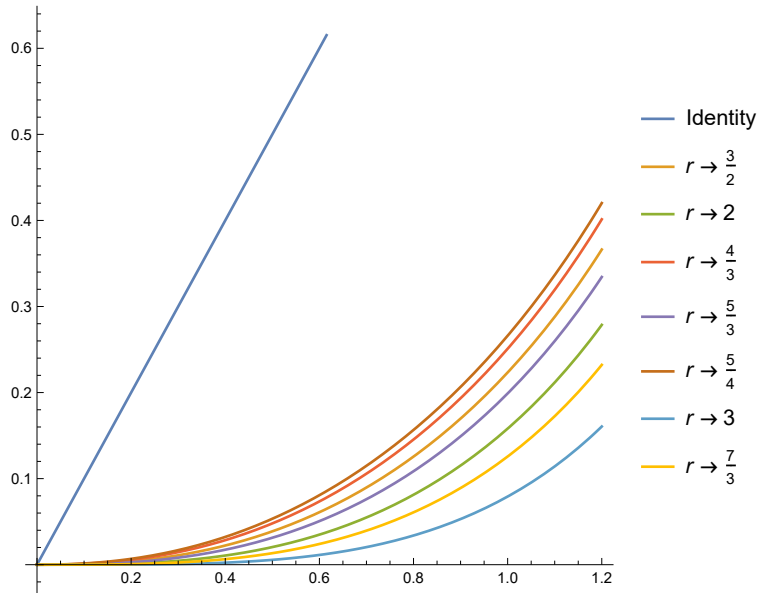

FIGURE 18. First return map: $m = 0$, $k = -1$, and $r < 1$.

FIGURE 19. First return map: $m = 0$, $k = -1$, and $r > 1$.
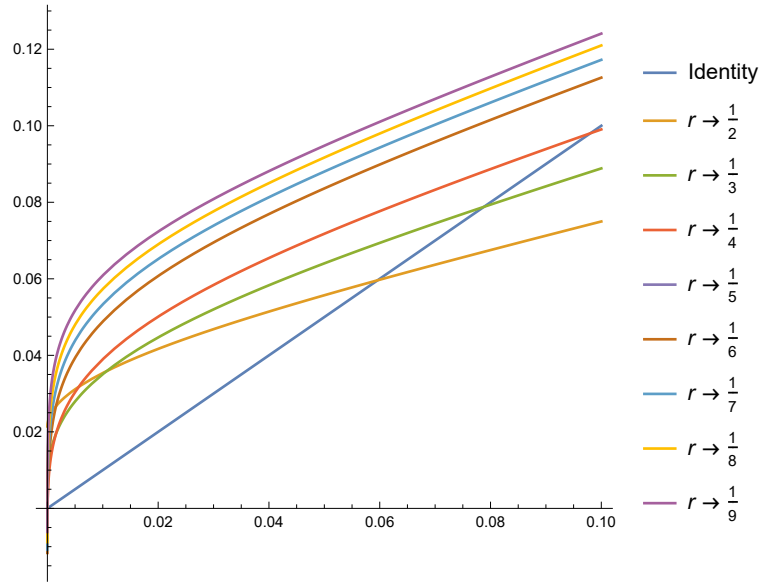
FIGURE 20. First return map: $m = -0.5$, $k = -1$, $d = 1.27$, and $r < 1$.
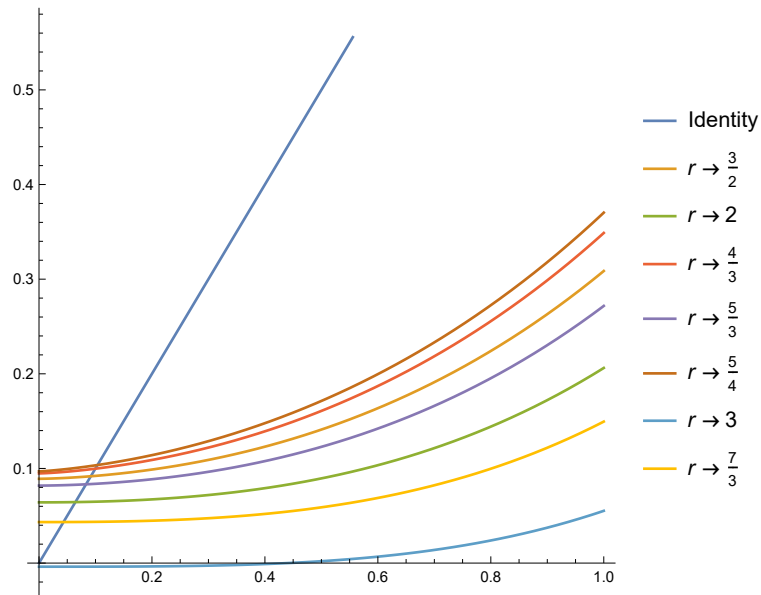
FIGURE 21. First return map: $m = -0.5$, $k = -1$, $d = 1.3$, and $r > 1$.
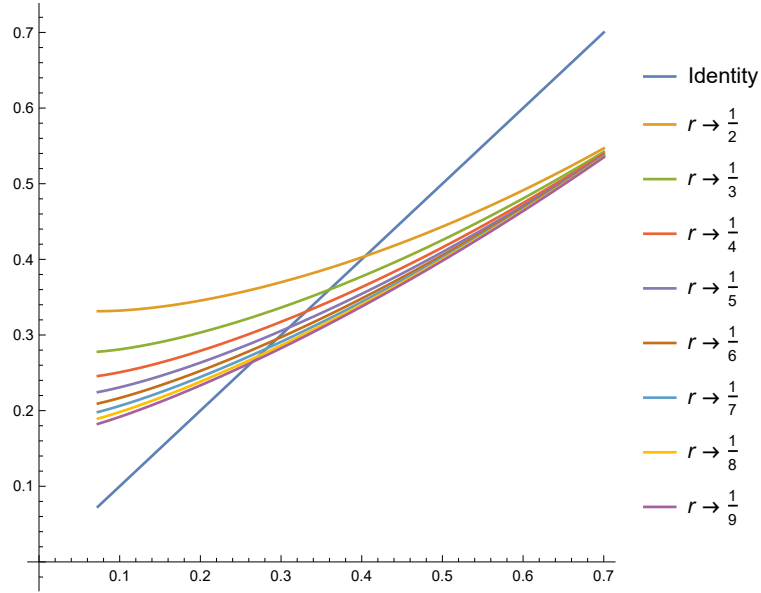
FIGURE 22. First return map: $m = 0.2$, $k = -1$, $d = 1.26$, and of $r < 1$.
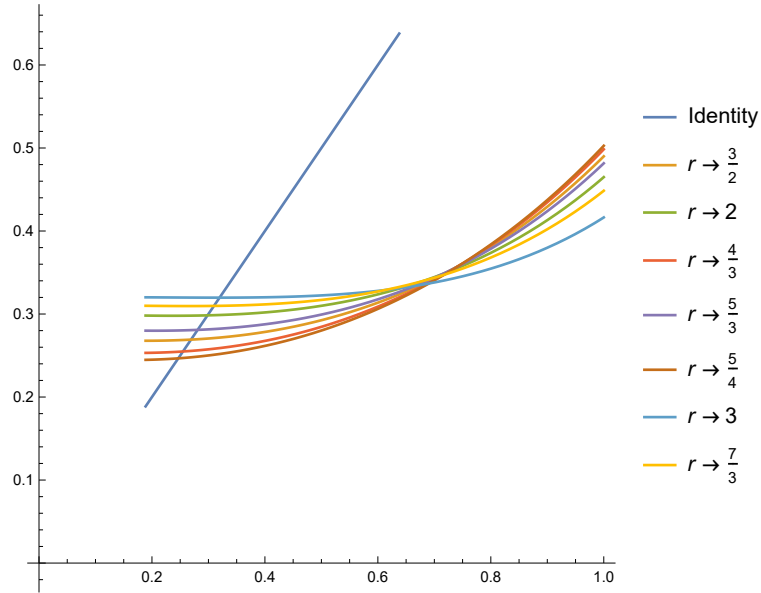
FIGURE 23. First return map: $m = 0.2$, $k = -1$, $d = 1.15$, and $r > 1$.

6. Application: a pendulum with on/off control

Consider the model for a simple pendulum with damping given by

$$(9) \qquad \begin{pmatrix} \dot{x} \\ \dot{y} \end{pmatrix} = \begin{pmatrix} y \\ a_1 y - \sin(x) \end{pmatrix} = X_{a_1}(x,y),$$

where x is the angle with the vertical axis, $y = \dot{x}$ is the angular speed and a_1 is a negative constant.

Let us then apply a control to the pendulum, in the form of an extra driving force, $a_2 \left(x + \frac{\pi}{2}\right) \frac{\partial}{\partial y}$, added to (9) if $\dot{x} < a_3 - a_4(x+\pi)$. The result is a nonsmooth system with nonsmooth vector field $Z_a = (X_{a_1}, Y_{a_1,a_2})$, with $a = (a_1, a_2, a_3, a_4)$, $\Sigma = \{(x,y) \in \mathbb{R}^2 ; y + a_4(x+\pi) = a_3\}$, and

$$Y_{a_1,a_2}(x,y) = \begin{pmatrix} y \\ a_1 y - \sin(x) + a_2 \left(x + \frac{\pi}{2}\right) \end{pmatrix}.$$

$S_X = (-\pi, 0)$ is a saddle point of X_{a_1}, with hyperbolicity ratio $r(a_1) = -\frac{a_1 - \sqrt{a_1^2 + 4}}{a_1 + \sqrt{a_1^2 + 4}}$. It is a real saddle when $a_3 < 0$, a boundary saddle when $a_3 = 0$, and a virtual saddle when $a_3 > 0$. For $a_3 \approx 0$ there exists a tangency point, in Σ, near S_X which we label P_{Z_a} and the first coordinate of this point will be denoted by p_a. The point P_{Z_a} coincides with S_X when $a_3 = 0$ and it is a fold point if $a_3 \neq 0$. A direct calculation gives that, for $x \approx p_a$, there exists a crossing region when $x > p_a$ and there is a sliding region when $x < p_a$.

This model realizes a degenerate cycle as studied in the previous sections. Some examples of trajectories are illustrated in Figure 24. These show that the unstable manifold of the saddle in Σ^+ meets Σ in the sliding region, after it passes through Σ^c, and the unstable manifold of S_X in Σ^+ meets Σ in the crossing region twice. It follows from continuity that Z_a presents a degenerate cycle through a saddle-regular point for $a_2 = -0.77$, $a_3 = 0$, $a_4 = 0.1$ and some $a_1 \in (-0.2, -0.1)$.
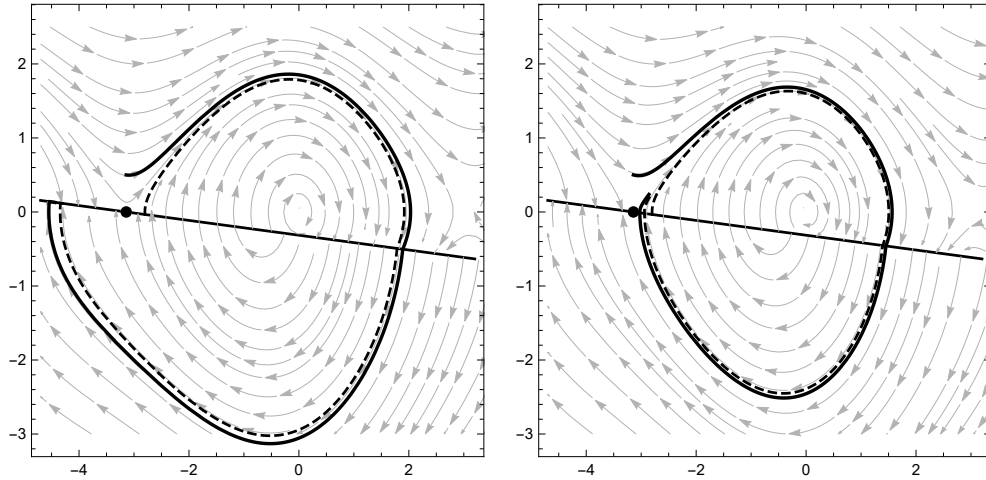

FIGURE 24. Trajectories of Z_a. Left hand side corresponds to $a = (-0.1, -0.77, 0, 0.1)$ and right hand side corresponds to $a = (-0.2, -0.77, 0, 0.1)$.

This system represents the case DSC_{11}, and realizes each one of the regions in the bifurcation diagram in Figure 11. For simplicity, let q_a be the first coordinate of the point Q_{Z_a} (near P_{Z_a}) which vanishes the sliding vector field, i.e., Q_{Z_a} is the pseudo-equilibrium point when it is in the sliding region.

- **Region R_1^1**

Consider the following values of parameters and initial conditions: $a = (-0.1, -0.77, 0.1, 0.1)$, $x_{01} = (-\pi, 05) \in \Sigma$, and $x_{02} = (-2.8, 0.1 - 0.1(\pi - 2.8)) \in \Sigma^+$. For these values $p_a = -3.14159\ldots$, $q_a = -2.14159\ldots$, $\pi_a(x_{01}) = -4.51446\ldots$, and $\pi_a(x_{02}) = -4.37873\ldots$. Since $q_a > p_a$, there is no pseudo-equilibrium point. The correspondent trajectories are shown in Figure 25. By continuity, the trajectory passing through S_X intersects Σ in the sliding region.
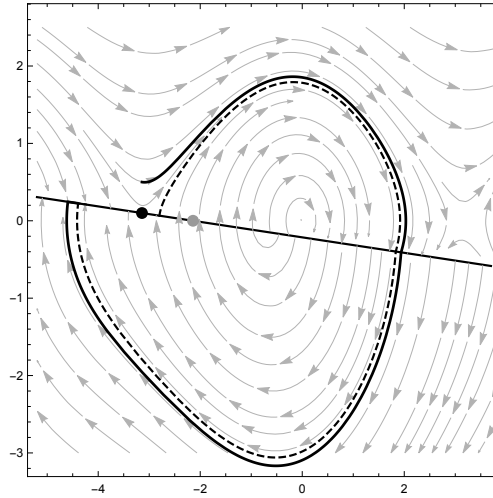
FIGURE 25. Trajectories of Z_a in R_1^1: $a = (-0.1, -0.77, 0.1, 0.1)$. The solid trajectory corresponds to to x_{01} and the dashed trajectory corresponds to to x_{02}. P_{Z_a} is the black point and Q_{Z_a} is the gray point.

- **Region R_2^1**

Considering the following values of parameters and initial conditions: $a = (-0.2, -0.77, 0.1, 0.1)$, $x_{01} = (-\pi, 0.5)) \in \Sigma^+$ and $x_{02} = (-2.5, 0.1 - 0.1(\pi - 2.5)) \in \Sigma$, we obtain $p_a = -3.13169\ldots$, $q_a = -2.14159\ldots$, $\pi_a(x_{01}) = -3.06627\ldots$ and $\pi_a(x_{02}) = -2.90533\ldots$. Since $q_a > p_a$ there is no pseudo-equilibrium point. These trajectories are shown in Figure 26. By continuity, the trajectory trough P_{Z_a} (which is a fold point) intersects Σ twice in the crossing region twice. These trajectories do not cross the sliding region near P_{Z_a}. We have $\pi_a((-3.1, 0.1 - 0.1(\pi - 3.1))) = -3.00766\cdots > -3.1$ and $\pi_a((-2.9, 0.1 - 0.1(\pi - 2.9))) = -2.9955\cdots < -2.9$, since the first return map is continuous, must exists an attracting limit cycle through a point $(x_c, 0.1 - 0.1(\pi + x_c))$ for some $x_c \in (-3.1, -2.9)$. See the graph of the first return map in Figure 27.
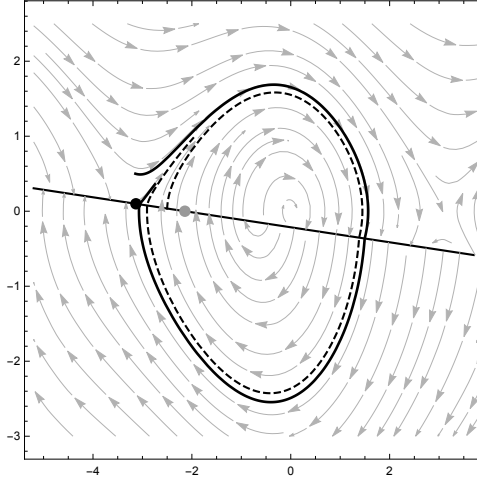
FIGURE 26. Trajectories of Z_a in R_2^1: $a = (-0.2, -0.77, 0.1, 0.1)$. The solid trajectory corresponds to to x_{01} and the dashed trajectory corresponds to to x_{02}. P_{Z_a} is the black point and Q_{Z_a} is the gray point.
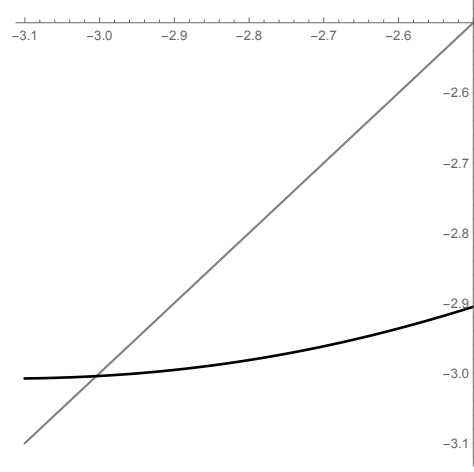
FIGURE 27. First return map in R_2: $a = (-0.2, -0.77, 0.1, 0.1)$. The origin is located in $(-2.5, -2.5)$.

- **Curve $\alpha^+ = \{(\alpha, 0); \alpha > 0\}$**

When $a_3 = 0$ the saddle point is on the boundary. For the values of parameters and initial conditions $a = (-0.2, -0.77, 0, 0.1)$, $x_{01} = (-\pi, 0.5)$, and $x_{02} = (-2.8, -0.1(\pi - 2.8))$ we obtain $p_a = q_a = -3.14159\ldots$, $\pi_a(x_{01}) = -3.02473\ldots$, and $\pi_a(x_{02}) = -2.93979\ldots$. These trajectories are illustrated in Figure 28. The unstable manifold of S_X in Σ^+ intersects Σ^c, at the second time, in a neighborhood of S_X. We have $\pi_a((-3.1, -0.1(\pi - 3.1))) = -2.96489\cdots > -3.1$ and $\pi_a((-2.9, -0.1(\pi - 2.9))) = -2.95331\cdots < -2.9$. Since the first return map is continuous, it implies in the existence of an attracting limit cycle through $(x_c, -0.1(\pi + x_c))$ for some $x_c \in (-3.1, -2.9)$. See the graph of the first return map in figure 29.

- **Region R_3^1**

Consider the values of parameters and initial conditions:
$a = (-0.2, -0.77, -0.1, 0.1)$, $x_{01} = (-\pi, 0.6) \in \Sigma^+$, and $x_{02} = (-2.9, -0.1 - 0.1(\pi - 2.9)) \in \Sigma^+$. We obtain $p_a = -3.15149\ldots$, $q_a = -4.14159\ldots$, $\pi_a(x_{01}) = -2.99339\ldots$, and $\pi_a(x_{02}) = -2.89616\cdots < -2.9$. These trajectories are shown in Figure 30. Hence, the unstable manifold in Σ^+ that intersects Σ at the crossing region must intersect Σ^c again near P_{Z_a}. We have $\pi_a((-3.1, -0.1(\pi - 3.1))) = -3.31943\cdots > -3.1$ then there exists an attracting limit cycle through $(x_c, -0.1 - 0.1(\pi + x_c))$ for some $x_c \in (-3.1, -2.9)$. See the graph of the first return map in Figure 31.
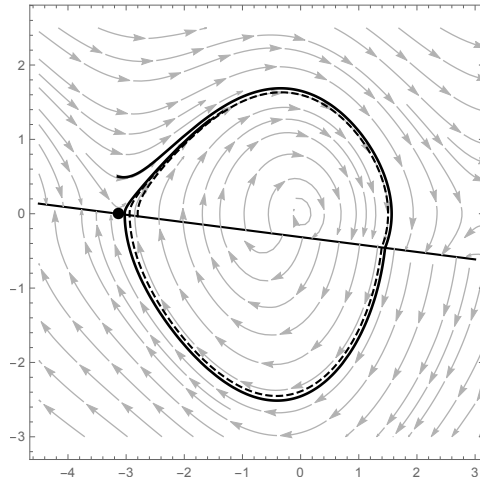
FIGURE 28. Trajectories of Z_a in α^+: $a = (-0.2, -0.77, 0, 0.1)$. The solid trajectory corresponds to to x_{01} and the dashed trajectory corresponds to to x_{02}. P_{Z_a} is the black point and Q_{Z_a} is the gray point.
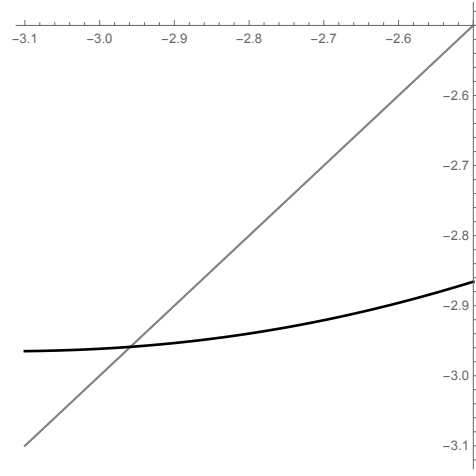

FIGURE 29. First return map in α^+: $a = (-0.2, -0.77, 0, 0.1)$. The origin of this axes is located at $(-2.5, -2.5)$.
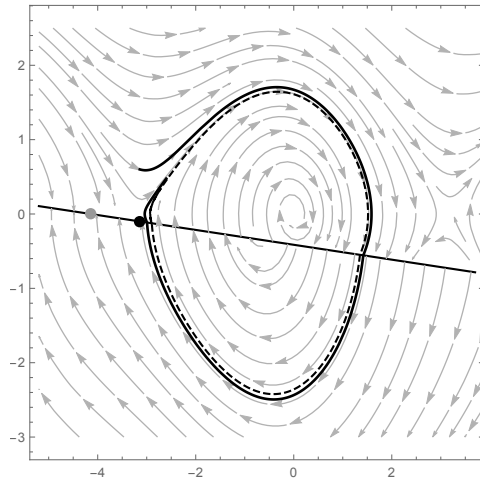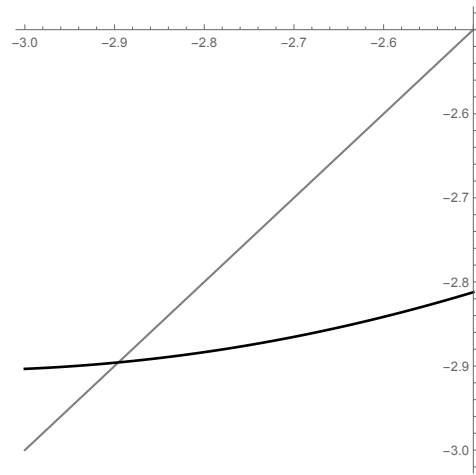

FIGURE 30. Trajectories of Z_a in R_3^1: $a = (-0.2, -0.77, -0.1, 0.1)$. The solid trajectory corresponds to to x_{01} and the dashed trajectory corresponds to to x_{02}. P_{Z_a} is the black point and Q_{Z_a} is the gray point.

FIGURE 31. First return map in R_3^1: $a = (-0.2, -0.77, -0.1, 0.1)$. The origin of this axes is located in $(-2.5, -2.5)$.

- **Region R_4^1**

Consider the values of parameters and initial conditions $a = (-0.185, -0.77, -0.2, 0.1)$, $x_{01} = (-\pi, 0.5) \in \Sigma^+$, and $x_{02} = (-2.8, -0.2 - 0.1(\pi - 2.8)) \in \Sigma$ we obtain $p_a = -3.15845\ldots$, $q_a = -5.14159\ldots$, $\pi_a(x_{01}) = -3.33481\ldots$, and $\pi_a(x_{02}) = -2.9545\ldots$. These trajectories are shown in Figure 32. The unstable manifold in Σ^+, which intersects Σ^c, reach the sliding region near P_{Z_a} after crossing through Σ at twice.

- **Regions $R_5^1 \cup \gamma_{x_1} \cup R_6^1$**

Consider the values of parameters and initial conditions $a = (-0.15, -0.77, -0.1, 0.1)$, $x_{01} = (-\pi, 0.5) \in \Sigma^+$, and $x_{02} = (-2.7, -0.1 - 0.1(\pi - 2.7)) \in \Sigma$ we obtain the values $p_a = -3.14657\ldots$, $q_a = -4.14159\ldots$, $\pi_a(x_{01}) = -3.57493\ldots$ and $\pi_a(x_{02}) = -3.41217\ldots$. These trajectories are shown in figure 33. The unstable manifold in Σ^+, which crosses Σ^c, intersects Σ^s at a point between the pseudo-equilibrium and the fold point.
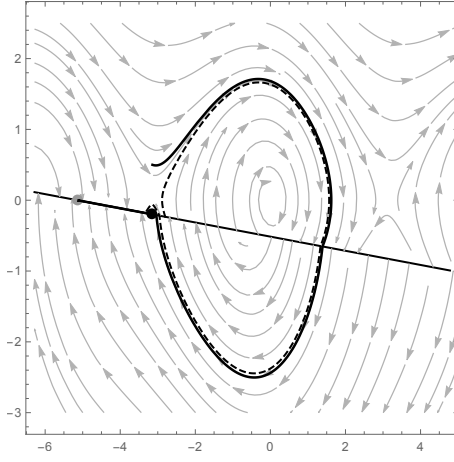

FIGURE 32. Trajectories of Z_a in R_4^1: $a = (-0.185, -0.77, -0.2, 0.1)$. The solid trajectory corresponds to to x_{01} and the dashed trajectory corresponds to to x_{02}. P_{Z_a} is the black point and Q_{Z_a} is the gray point.
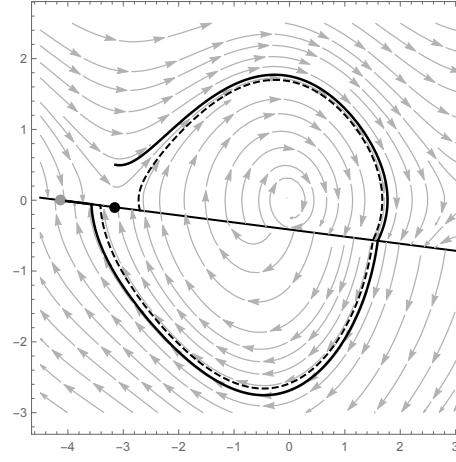
FIGURE 33. Trajectories of Z_a in $R_5^1 \cup \gamma_{x_1} \cup R_6^1$: $a = (-0.15, -0.77, -0.1, 0.1)$. The solid trajectory corresponds to to x_{01} and the dashed trajectory corresponds to to x_{02}. P_{Z_a} is the black point and Q_{Z_a} is the gray point.

- **Region R_7^1**

Consider the values of parameters and initial conditions $a = (-0.1, -0.77, -0.1, 0.1)$, $x_{01} = (-2.9, -0.1 - 0.1(\pi - 2.9)) \in \Sigma^+$, and $x_{02} = (-2.9, -0.1 - 0.1(\pi - 2.9)) \in \Sigma^+$. So, $p_a = -3.14159\ldots$, $q_a = -4.14159\ldots$, $\pi_a(x_{01}) = -4.46432\ldots$, and $\pi_a(x_{02}) = -4.30114\ldots$. These trajectories are shown in figure 34. The branch of the unstable manifold in Σ^+, which crosses Σ transversely in Σ^c, intersects Σ^s at a point P_7 such that the pseudo-equilibrium is located between P_7 and P_{Z_a}.

- **Curve** $\alpha^- = \{(\alpha, 0); \alpha < 0\}$

Considering the values of parameters and initial conditions $a = (-0.1, -0.77, 0, 0.1)$, $x_{01} = (-\pi, 0.5) \in \Sigma^+$, and $x_{02} = (-2.8, -0.1(\pi - 2.8)) \in \Sigma$ we obtain $p_a = q_a = -3.14159\ldots$, $\pi_a(x_{01}) = -4.54177\ldots$ and $\pi_a(x_{02}) = -4.33775\ldots$. These trajectories are shown in Figure 35. So, the unstable manifold in Σ^+ crosses Σ^c once before it reaches Σ^s.
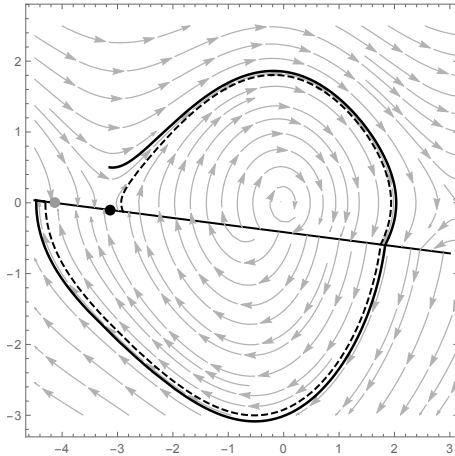

FIGURE 34. Trajectories of Z_a in R_7^1: $a = (-0.1, -0.77, -0.1, 0.1)$. The solid trajectory corresponds to to x_{01} and the dashed trajectory corresponds to to x_{02}. P_{Z_a} is the black point and Q_{Z_a} is the gray point.
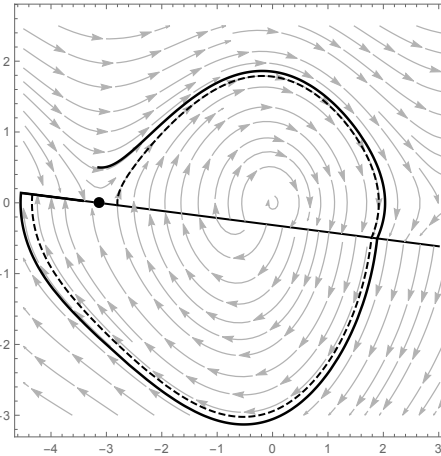
FIGURE 35. Trajectories of Z_a in α^-: $a = (-0.1, -0.77, 0, 0.1)$. The solid trajectory corresponds to to x_{01} and the dashed trajectory corresponds to to x_{02}. P_{Z_a} is the black point and Q_{Z_a} is the gray point.

7. Closing Remarks

We have unfolded the homoclinic connection to a boundary saddle in nonsmooth dynamical system. The local transition between regular saddle off and pseudo-saddle on the switching surface, and the global bifurcation of periodic orbits from the homoclinic orbit, create a complicated bifurcation structure. It would be worthwhile to improve the results by studying those bifurcations taking account the cyclicity of limit cycles bifurcating from a homoclinic boundary-saddle connection in the nonsmooth context, [6] can be seen as a guideline to this problem.

We have presented the bifurcation diagrams for non-resonant saddles only. The application to a forced pendulum demonstrates how readily these bifurcations appear in practical control scenarios.

8. Acknowledgments

References

[1] Y. A. Kuznetsov, S. Rinaldi, A. Gragnani, One-parameter bifurcations in planar Filippov systems, Int. J. Bifurc. Chaos 13 (2003) 215–218.

[2] M. Bernardo, C. Budd, A. R. Champneys, P. Kowalczyk, Piecewise-smooth dynamical systems: theory and applications, Vol. 163, Springer Science & Business Media, 2008.

[3] A. F. Filippov, Differential equations with discontinuous right-hand sides: control systems, Mathematics and its Applications. Soviet Series, Kluwer Academic Publ, Dordrecht, 1988.
URL http://opac.inria.fr/record=b1120770

[4] M. Guardia, T. M. Seara, M. A. Teixeira, Generic bifurcations of low codimension of planar Filippov systems, J. Differential Equations 250 (4) (2011) 1967–2023. doi:10.1016/j.jde.2010.11.016.
URL http://dx.doi.org/10.1016/j.jde.2010.11.016

[5] M. A. Teixeira, Generic bifurcation in manifolds with boundary, Journal of Differential Equations 25 (1) (1977) 65–89.

[6] R. Roussarie, Bifurcation of planar vector fields and Hilbert's sixteenth problem, Springer, 1998.

[7] A. A. Andronov, A. A. Vitt, S. E. Khaikin, Theory of oscillators, Translated from the Russian by F. Immirzi; translation edited and abridged by W. Fishwick, Pergamon Press, Oxford-New York-Toronto, Ont., 1966.

[8] N. Minorsky, T. Teichmann, Nonlinear oscillations, Physics Today 15 (9) (2009) 63–65.

[9] E. A. Barbashin, Introduction to the Theory of Stability, Wolters-Noordhoff, 1970.

[10] P. T. Cardin, T. De Carvalho, J. Llibre, Limit cycles of discontinuous piecewise linear differential systems, International Journal of Bifurcation and Chaos 21 (11) (2011) 3181–3194.

[11] A. Colombo, M. Di Bernardo, S. Hogan, M. Jeffrey, Bifurcations of piecewise smooth flows: Perspectives, methodologies and open problems, Physica D: Nonlinear Phenomena 241 (22) (2012) 1845–1860.

[12] O. Makarenkov, J. S. W. Lamb, Dynamics and bifurcations of nonsmooth systems: a survey, Physica D: Nonlinear Phenomena 241 (22) (2012) 1826–1844.

(KSA) Department of Mathematics, UFG, IME, Goiânia-GO, 74690-900, Brazil
E-mail address: kamila.andrade@ufg.com

(MRJ) Engineering Mathematics, University of Bristol, Merchant Venturer's Building, Bristol BS8 1UB, UK
E-mail address: mike.jeffrey@bristol.ac.uk

(RMM) Department of Mathematics, Unicamp, IMECC, Campinas-SP, 13083-970, Brazil
E-mail address: rmiranda@ime.unicamp.br

(MAT) Department of Mathematics, Unicamp, IMECC, Campinas-SP, 13083-970, Brazil
E-mail address: teixeira@ime.unicamp.br